Image Restoration using Adaptive Soft Computing Techniques

Ph.D Thesis

Muhammad Nadeem
Reg. No. 145-FBAS/PHDCS/F16

Supervisor
Dr. Ayyaz Hussain
Associate Professor

Department of Computer Science & Software Engineering
Faculty of Basic and Applied Sciences
International Islamic University, Islamabad, Pakistan
2020

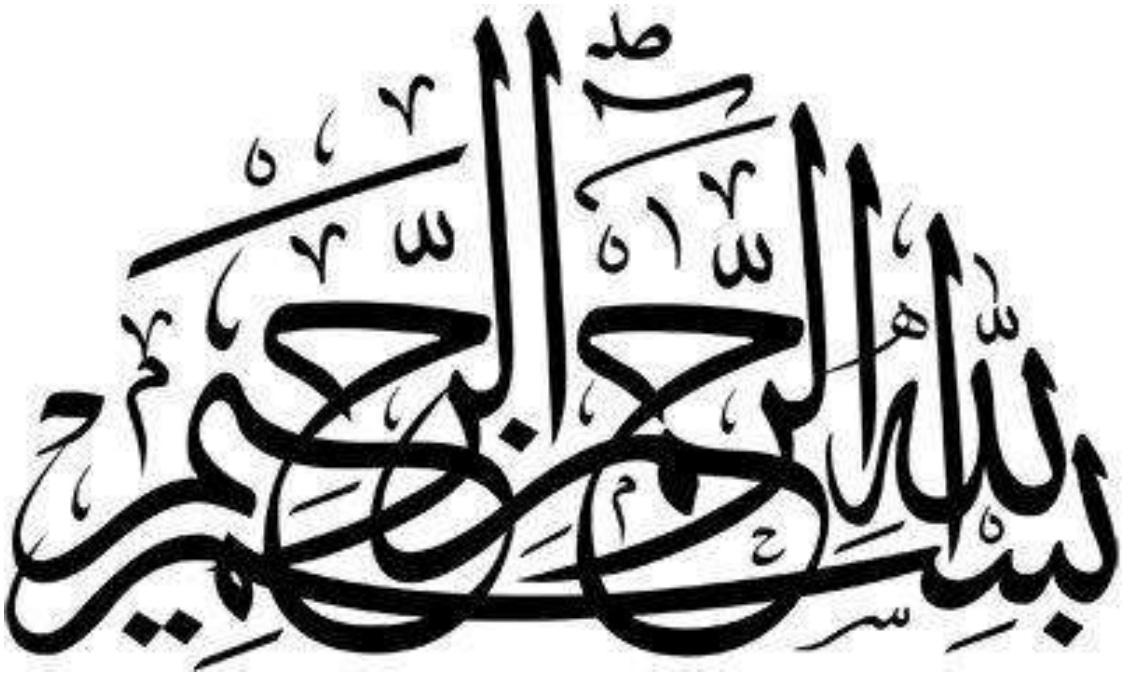

Acknowledgment

I would love to bow my head before Allah Almighty, the Most Gracious, and the Most Merciful, whose countless blessings bestowed upon me throughout my life and especially during the whole course of my Ph.D.

I would like to extend my special thanks of gratitude to my kind-hearted supervisor "***Dr. Ayyaz Hussain***", Associate Professor, for his able guidance and support in the completion of my research work.

Next, I owe my genuine gratefulness to my parents, wife, children, and other family members, without their sincere prayers, I would not have reached this point.

I am also thankful to all my colleagues, friends, and other persons who have directly or indirectly helped me in the completion of my research work.

Declaration

I, Muhammad Nadeem, hereby state that my Ph.D thesis titled "***Image Restoration using Adaptive Soft Computing Techniques"*** is my own work except where due reference is made in the text and it has not been previously submitted by me for taking partial or full credit for the award of any degree at this university or anywhere else in the world. If my statement is found to be incorrect, at any time even after my graduation, the university has the right to revoke my Ph.D degree.

Muhammad Nadeem

145-FBAS/PHDCS/F16

Dedication

To My:

Parents Abba G, Amma G (Late), Wife,

Kids: Sami, Haseeb, and Saad,

Brothers & Sister,

Friends,

and

Teachers

Abstract

Generally, real-time images are frequently degraded by various kinds of noise sources. Consequently, succeeding image operations such as image segmentation, object detection and tracking may perform poorly in the presence of noise. So the restoration of noisy images is an active and highly demanded area of research as previous information about noise is almost unknown in many cases making image restoration a more difficult and challenging job. Noise removal is a fundamental step that plays a vital and challenging role in the area of signal and image processing.

This research is an attempt to suppress low and high categories of two types of noises i.e., ***Impulse noise*** present in almost every image and ***Speckle noise*** from ultrasonic data in such a manner to enhance the relevant image content. For this, unsupervised filtering techniques based on statistical and widely used soft computing technique – fuzzy logic, are applied to suppress the impulse and speckle noise hence improving its quality for subsequent image processing operations specifically for diagnostic purposes.

In this thesis, the following contributions have been made in the domain of **Image Restoration (IR)**. In the first phase, an efficient image restoration technique, Quadrant based Spatially Adaptive Fuzzy filter based on spatially linked directional adjoining pixels and fuzzy logic for addressing moderate and highly corrupted grayscale images with the challenging type of impulse noise that is Random Valued Impulse Noise (RVIN) is presented. The proposed technique decomposes a larger sized impulsive region of an image into numerous overlapping small patches for the estimation of lower as well as a higher degree of impulse noise, with enhanced image restoration results.

In the second phase, an innovative Fuzzy logic based Non-Local Mean filter is introduced in this thesis to model the speckle noise and to restore the degraded image using Fuzzy Uncertainty Modelling (FUM), smoothed by local statistic based information with the capability of retaining the fine details present in the low as well as highly speckled ultrasound images.

Objective analysis performed using popular quantitative measures and subjective evaluation of the results show the efficacy of the proposed filters over most of the bench-marked denoising filters in removing impulse as well as speckle noise while retaining the edges and other important details present in the image.

Table of Contents

List of Figures

List of Tables

List of Abbreviations

ACWM	Adaptive Centre Weighted Median
AD / SRAD	Anisotropic Diffusion/Speckle Reducing Anisotropic Diffusion
ADWM	Adaptive Dynamically Weighted Median
AFIDM	Adaptive Fuzzy Inference System based Directional Median
AFT-IF	Adaptive Fuzzy Transform-based Image Filter
ANFIS	Adaptive Neural Fuzzy Inference System
ANN	Artificial Neural Network
ATFDF	Adaptive Threshold based Fuzzy Directional Filter
CAD	Computer-Aided Design
CEF	Contrast Enhancement-Based Filter
DL	Deep Learning
DPC-INR	Dissimilar Pixel Counting based Impulse Noise Removal
DWM	Directional Weighted Median
FCM	Fuzzy c-Means clustering
FIDRM	Fuzzy Impulse Noise Detection and Reduction Method
FRDM	Fuzzy Reasoning based Directional Median
FSVM	Fuzzy Support Vector Machine
FUM	Fuzzy Uncertainty Modelling
GA / GP	Genetic Algorithm / Genetic Programming
HFF	Histogram-based Fuzzy Filter
HVS	Human Visual System
IN / RVIN	Impulse Noise / Random Valued Impulse Noise
IR	Image Restoration
LBP	Local Binary Pattern
LLMMSE	Local Linear Minimum Mean Square Error
MDW	Modified Directional Weighted filter
ML / EC	Machine Learning / Evolutionary Computing
MSE	Mean Square Error
MSM	Multi-State Median
NLM	Non-Local Mean

NLMLS	Non-local Mean filter combined with Local Statistics
NWM	New Weighted Mean filter
OBNLM	Optimized Bayesian Non-Local Mean
PDE	Partial Differential Equation
PWMAD	Pixel-Wise Mean Absolute Difference
ROAD	Rank Ordered Absolute Difference
ROD-ROAD	Rank Ordered Absolute Difference
SBF	Squeeze Box Filter
SC / FL	Soft Computing / Fuzzy Logic
SDOOD	Standard Deviation for Obtaining the Optimal Direction
SNR / PSNR	Signal-to-Noise Ratio / Peak Signal-to-Noise Ratio
SPN	Salt & Pepper Noise
SRBF	Speckle Reducing Bilateral Filter
SSIM / FSIM	Structured Similarity Index Measure / Feature SIM
TF	Trilateral Filter
US	Ultrasound

Research Contribution

The following research papers related to this thesis are published in international journals during the course of Ph.D. research.

1. **M. Nadeem**, Ayyaz Hussain, Asim Munir et al., "Removal of random valued impulse noise from grayscale images using quadrant based spatially adaptive fuzzy filter", Signal Processing, **Elsevier**, Volume 169, **2020**, 107403. (**IF: 4.086)**

2. **M. Nadeem**, Ayyaz Hussain, Asim Munir, "Fuzzy logic based computational model for speckle noise removal in ultrasound images", Multimedia Tools and Applications (MTAP), **Springer**, Volume 78, Issue 13, pp 18531–18548, July **2019**. (**IF: 2.101)**

Chapter 1

Introduction

Chapter 1

1. Introduction

It is an obvious fact that images contain some of mankind's most valuable information. More than a single two–dimensional representation of signal intensity, images elicit feelings, inspire new thinking and record historical events [1]. Not surprisingly, considerable research has been dedicated to the analysis and manipulation of images, known broadly as image enhancement, image restoration, image segmentation, image recognition, watermarking, super-resolution, image coding, etc. Furthermore, images can be processed as sequences for video tracking, motion estimation and computer vision. The main focus of this thesis is in the area of "***Image Restoration***" of digital images.

1.1 Image Restoration: Background and Motivation

Digital Image Restoration is a process that intends to eliminate the degradations (noise and other type of distortions) introduced during image acquisition, with the objective to generate a more closure, clearer and fairer picture of the original scene. In digital images noise (unwanted information) is often added due to transmission errors, acquisition problems and storage because of sensors with noise particles and imperfections in communication or transmitting channels [2,3]. In noise added images, compatibility of the pixels having noise becomes compromised with their resident neighboring pixels.

Research into image restoration techniques first became popular in the 1950s and 1960s among the scientists involved in space exploration. The high cost and effort required to launch a man into space made any images that were captured on the mission extremely valuable to scientists. Unfortunately, due to the harsh environments of space and the limitations of imaging technology, images were often degraded. As a consequence, research into image restoration methods grew rapidly and soon spread to

other areas such as medical analysis, remote sensing, astronomy, and aerial exploration [4–7], etc. Medical imaging has benefited enormously from restoration methods, which provide a means of obtaining more accurate images for improved patient diagnosis [8].

1.2 Noise Types

Digital images might be exposed to various types of noise sources. These noises could be categorized into dependent and independent noise types.

1.2.1 Independent Noise

This is the type of noise in which the noise is independent of signal's data (image). The example is additive noise in which the resultant image obtained after the degradation process is the addition of both, real (true) values and degraded values (pixels). A corrupted image $g_n(r,c)$ is acquired when the additive noise $\eta_n(r,c)$ and degradation function $h_d(r,c)$ operate simultaneously on an input image $f_o(r,c)$ and can be represented as:

$$g_n(r,c) = f_o(r,c) * h_d(r,c) + \eta_n(r,c) \quad (1.1)$$

When an image contains only additive noise $\eta_n(r,c)$ degradation, then Eq. 1.1 changes to:

$$g_n(r,c) = f_o(r,c) + \eta_n(r,c) \quad (1.2)$$

A digital image is a composition of high and low-frequency components. Low-frequency components correspond to the smooth regions inside the image while high-frequency components correspond to highly variations such as lines or edges. Additive noise is generally extended (distributed) evenly over the frequency domain (*white noise*). The noise affects high-frequency components mostly which can be removed or reduced by using different types of *"low-pass"* filters in frequency or spatial domain. As spatial filters are computationally robust than frequency domain filters [2], they are preferred.

1.2.2 Dependent Noise

The second type of noise is the *data-dependent noise* which arises when "monochromatic radiation is scattered from a surface whose roughness is of the order of a wavelength, causing wave interference which results in image - *speckle*" [2]. This noise is modeled with a multiplicative or non-linear model, mathematically more complicated. Image dependent noise is given by:

$$g_n(r,c) = f_o(r,c)\,\eta_n(r,c) \qquad (1.3)$$

Image may get tainted with other noise types as well such as Gaussian noise, shot noise, heavy-tailed noise, anisotropic noise, quantization, and uniform noise, etc.

The research work presented in this thesis focuses on the most challenging type of impulse noise i.e., **Random Valued Impulse Noise** present in almost all images and **Speckle noise** affecting the ultrasonic images. This research work contributes to the field of image processing in general and image restoration in particular. Most of the existing statistical and rule-based algorithms developed in this domain are either less intelligent or of static nature. Non-linear adaptive techniques outperform traditional linear techniques but still lag behind in many cases to solve the classical image restoration problems.

1.3 Soft Computing Techniques

Soft Computing contrasted with traditional hard computing deals with "approximate models" and give solutions to "complex real-life problems". Unlike the algorithmic type of hard computing, soft computing deals with uncertainty, imprecision, partial truth and approximation to achieve tractability, robustness and low solution cost [9]. Actually, the basic idea of SC is taken from the study and working of the human mind. Fuzzy logic, Genetic algorithms, artificial neural networks, machine learning and evolutionary computing are examples of the techniques based on soft computing. Even though soft computing methods had been first presented in the late 1980s, it has now emerged as a primary and hot research area in the discipline of computer science.

Due to the nature and adaptiveness of soft computing techniques, researchers are using them successfully in almost all areas related to domestic, industrial and commercial areas. With the advancements of the IT industry and its usage in different fields, it is a fact that the application areas of soft computing will continue to widen and grow in the future. Components of soft computing include:

- Fuzzy Logic
- Neural Networks
- Evolutionary Computation
- Machine Learning

A brief introduction of these components is given below.

1.3.1 Fuzzy - Soft computing technique

Professor Zadeh introduced the fuzzy theory [10–12], a method for "*representing human knowledge that is imprecise by nature*". Zadeh was in the belief that "*people do not require precise, numerical input, and yet they are capable of highly adaptive control*". Compared to the conventional Boolean type of logic (0 or 1), fuzzy logic been extended to deal with the concept of partial truth i.e., truth-values between "completely-true (1)" and "completely-false (0)". The basic configuration model of a fuzzy rule-based system is shown in Fig. 1.1. The crisp numerical value coming from the existing sensor is input to the fuzzification interface which transforms it into a fuzzy linguistic value. These fuzzy values are taken by the inference engine as input and after processing through the fuzzy-rule-base (*IF-THEN* rules involving linguistic variables), generate fuzzy outputs. Defuzzification is the last step of the fuzzy logic system which produces the crisp output value back from the fuzzy value.

Why select fuzzy logic?

It allows the designer to characterize the intended behavior of the system with the help of simple "*IF-THEN*" relations. In many application areas, the use of this logic gives a simplified solution that takes less design time. Furthermore, fuzzy logic-based solutions are very easy to validate, verify and optimize due to its simplest logic. A more powerful solution can be offered to complex problems by combining the conventional

methods and artificial neural networks combined with fuzzy based logic. Fuzzy rule-based logic provides an approach to *approximate reasoning* in which the rules of inference are *approximate* rather than *exact*. These systems are very useful and effective in handling incomplete, imprecise and unreliable types of information. Due to the rule-based nature of the fuzzy system, any rational number of input values can be processed and multiple outputs can be produced.

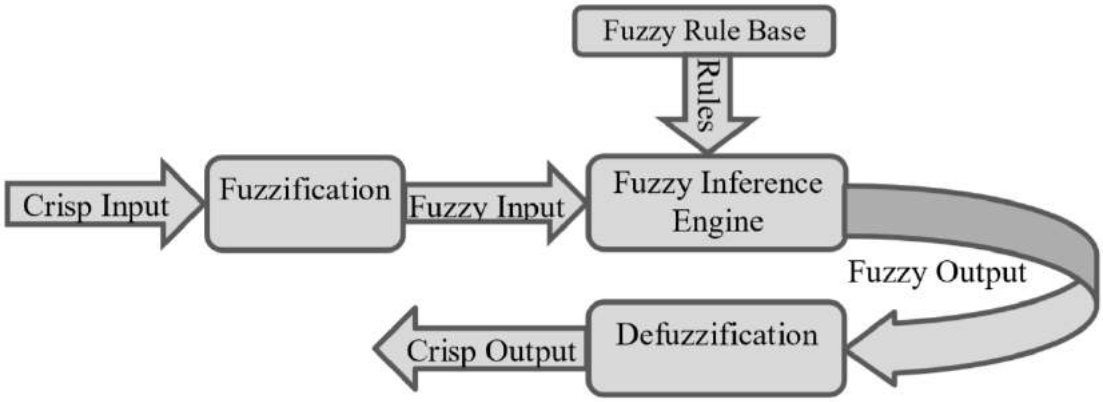

Fig. 1.1: Architecture of fuzzy-based system

1.3.2 Neural Networks – Soft Computing Technique

Artificial neural networks [13] is one of the fast-growing research field in the discipline of computer science and engineering. Artificial neural networks are "*information processing systems"* inspired by the concept of natural *"biological nervous system"* and the working of the *"brain"*. These artificial networks are usually configured for specific applications, such as image processing, image compression, watermarking, data and pattern recognition, stock market and weather prediction, etc. The neural network aims to bring "*traditional computers*" a bit closer to the way "*human brain*" works. The working efficiency of ANNs is directly dependent upon the non-linearity nature of the relationship between the inputs and outputs. ANN is a large network of interconnected elements called nodes based on the concept of human neurons. Each node/neuron performs a little operation and the overall operation is the weighted sum of these operations. In the initial stage, NNs are trained by feeding with a huge amount of data, that's how they start learning. There are many learning strategies namely supervised, unsupervised and reinforcement learning. Supervised learning is

used in a situation when a sample input dataset with known output is available. Unsupervised learning comes to an action when there is no input data set with known results. Reinforcement learning is a strategy built based on observation, in which the decision of NN is based on its environment.

An ANN consists of three layers namely input, hidden and output layer. These three layers are composed of several nodes that behave like neurons. These nodes are connected by links (wires) provides a way of communication with other nodes of the network as shown in Fig. 1.2. The first layer receives input in the form of raw data. Every subsequent layer receives the output of the previous layers as an input, processes it and sends the output to the next layer. The final layers generate the output. To train the network, mostly the backpropagation algorithm is used in many cases. In this type of algorithm, the desired output and output generated by the ANN are compared. In case the output of the ANN is not as desired, the *"weights"* between the layers are updated and the process is repeated until the error value becomes very small.

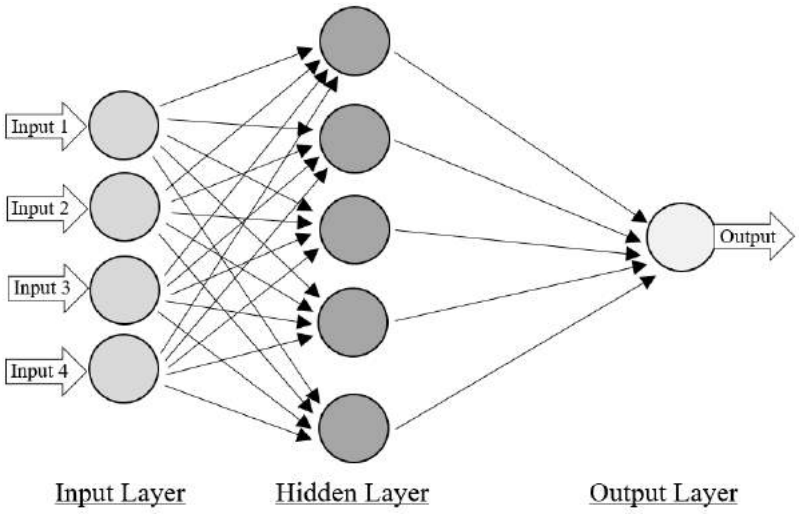

Fig. 1.2: Architecture of Artificial Neural Network

Limitations of Neural Networks:

- Computationally very expensive, as ANN requires excessive training in complex systems.
- Need a huge amount of data set.
- Not a universal tool for solving problems as there is no defined type of methodology for training and verifying an NN.

- The results of ANNs are greatly dependent on the accuracy of the available data.

1.3.3 Evolutionary Computation – Soft Computing Technique

Evolutionary Computation [14] based on Darwinian principles for automated problem solving, introduced by L. J. Fogel in the 1950s, is a major research area for adaptation and optimization. In the domain of computer science and engineering, EC is a technique of soft computing that involves combinatorics types of optimization problems. Such processes are often inspired by *"biological mechanisms of evolution*". EC uses evolutionary techniques which are evolutionary algorithms (genetic algorithms), swarm intelligent techniques (Ant Colony Optimization, Particle Swarm Optimization, etc.), etc.

1.3.3.1 Evolutionary Algorithms

EA is a subset of evolutionary computation methods that are generally inspired by biological evolution such as mutation, reproduction, recombination and selection [114]. Candidate solutions to the optimization problem play the role of individuals in a population, and the cost function determines the environment within which the solutions "*live*". The evolution of the population then takes place after the repeated application of the above-mentioned operators.

1.3.3.2 Evolutionary Algorithm Techniques

Some of the EA techniques are briefly discussed as under:

- **Genetic algorithm:** GA [13] is the most popular and belongs to the larger class of EA. It is used to generate the best solution to optimization problems using bio-inspired operators named mutation, crossover, and mutation.
- **Genetic programming:** It is a technique in which the programs are evolved from their unfit versions, and their fitness is determined by their ability to solve a computational problem.
- **Evolutionary programming:** The base of EP [14] is the same as that of genetic programming, but the structure of the program to be optimized is fixed and its numerical parameters are allowed to evolve.

1.3.4 Machine Learning – Soft Computing Technique

The process through which a system improves its performance from experience is called *"Learning"* [15]. So, Machine Learning is a term associated with *"computer programs"* that improve their performance automatically through experience. ML is required to produce systems that are overly complicated or become expensive to construct manually because they require specific thorough skills or complete knowledge of a specific task. It is very much needed in today's era because of the increasing volume of incoming data, an increase in computational power, growing progress in available algorithms and theories developed by the researchers and increasing support from all kinds of industries.

Applications of ML:

Handwriting recognition, information retrieval, machine perception, optimization, sentiment analysis, speech recognition, DNA sequence, natural language processing, medical diagnosis, etc.

1.4 Image Restoration using Fuzzy Logic

The field of image restoration has no exact and precise mathematical relationships between the input and output variables. Furthermore, the IR has uncertain nature in the noise detection phase and filtering phase.

So by its very nature, among all the soft computing techniques, **Fuzzy logic** is a perfect technique that can be used or can be merged with top-of-the-line restoration techniques for efficient detection of noise and restoration. This technique has found its application in around all domains of engineering and computer science fields.

The basic role of the fuzzy inference system (soft computing technique) in the image denoising process is to detect the pixels tainted with noise and to recover the noise-free pixel value from its degraded version.

1.5 Applications of IR

Image Restoration has a wide range of applications in the areas where the images are acquired, used and processed. Some examples of the areas where IR can be used or helpful are given as under:

- **Medicine:** X-rays [16], CT-Scan, MRI (Magnetic Resonance Imaging) [5], PET (Positron Emission Tomography) [17] and CAD (Computer-Aided Design) [18]). Noise-free images not only improve patient's diagnosis but also remove classic Poisson distribution of signal-dependent film grain noise in mammograms and chest X-rays.
- **Forensics:** In identifying physiological characteristics such as iris [19], face [20], and fingerprints [21], etc.
- **Remote Sensing:** Meteorological applications such as weather forecasting, locating natural resources–forests, water, etc.
- **Communication:** Videoconferencing, Watermarking [22], etc.
- **Industry automation:** Automated visual inspection in aerospace, food, textile, etc.
- **Traffic control:** Analyzing pictures taken by cameras for crowd control [23,24].
- **Defense:** Night vision devices, RADAR [25], etc.
- **Robotics:** Pilot-less vehicles, surface measurements [26], etc.

Several complicated problems [27–29] have been solved using soft computing techniques. Fuzzy logic, a branch of soft computing has gained much popularity in the latter half of this century due to its computational capabilities. Plenty of work has already been contributed in the field of IR using fuzzy logic but improvements are still required due to varying system requirements.

1.6 Problem Statement and Research Questions

As discussed, the main purpose of the image restoration process is to reconstruct or recover a deteriorated image to its original shape using some foreknowledge of

degradation phenomena and the original image. It is essential to refer here that apart from the recent advancements in imaging technology still, images suffer from many possible degradations like blur, motion, and noise.

In image processing, digital images may be contaminated with impulse and speckle devastates the uniformity between the adjoining pixels in the original image and may severely hamper subsequent image operations like segmentation, classification, tracking object, edge detection [4–6], etc. Therefore, the amount of noise present in a given image needs to be significantly reduced while retaining the original details such as lines, edges and textures.

An impulsive noise has an inherent property that is different from other types of noises like Gaussian noise that, affects only a subset of the image pixels leaving all other pixel values unaltered. Based on the distribution, impulse noise has usually two types: fixed valued (also termed as salt & pepper noise) [30] and **random valued impulse noise** [31]. In literature, many simple and complex denoising techniques have been developed for the effective exclusion of impulse noise from gray [32–34] as well as colored [35–37] images. These techniques perform very well for SPN but fail in handling RVIN effectively.

Unlike other non-invasive imaging techniques, ultrasound images are playing a vital role in medical diagnostics to visualize and examine the internal human body structures due to its portability, substantially cost-effective nature and harmless ionizing radiations. During the acquisition or transmission process, these images may corrupt by a multiplicative type of **speckle noise** [8,38]. Speckle is a granular noise that inherently reduces the image quality resulting in complications for the detection of small edges and other textural details. A considerable amount of research attention has been received in recent years but no one convincingly claims to have solved the problem satisfactorily.

In switching based image restoration, the noise filtering phase is substantially dependent on the accuracy and effectiveness of the noise detector. Most of the existing directional, linear, non-linear, NLM and other soft computing based noise detectors do not use the correct size of processing windows and the best statistical features present

among the adjoining pixels that reduce the accuracy of noise detectors which ultimately affects the efficiency of image restoration technique.

A large number of applications use human-reasoning and fuzzy logic-based solutions to complex problems. Most of the existing fuzzy techniques make their decisions using static threshold which leads to misclassification of noisy or edge pixels because data patterns of noise and image are usually not alike.

1.6.1 Research Questions

Following research questions/open issues have been extracted during the literature review:

1. How we can design or improve the noise detection process that can address low as well as high noise densities using soft computing techniques?
2. How soft computing techniques can be used to set the threshold adaptively in noise detection phase?
3. How we can improve the efficiency of the noise filtering phase using local context at changing the behavior of noise and image data for smoother performance?
4. How we can use quadrant based clustering methodology using fuzzy logic for better noise estimation and to enhance the edge preservation capabilities of the restoration technique.
5. A Local Linear Minimum Mean Square Error [39] estimator is a renowned ultrasonic denoising filter. This estimator uses local statistical features such as the variance, mean and mean-square values of the local neighborhood. How we can improve the performance of the existing LLMMSE estimator using non-local statistics and fuzzy logic?
6. How we can design filtering techniques that are efficient in noise detection and restoration and also are computationally inexpensive?

1.7 Research Contributions

The following novel contributions have been made in the field of Image Restoration during the research work carried out for this thesis:

- In **chapter 3**, a robust switching scheme based on soft computing technique (fuzzy logic) and statistical parameter estimation is proposed that uses the divide and conquer strategy to deal with low as well as the high degree of impulse noise present in the image.

  Fuzzy logic-based rules are exercised to categorize the impulsive pixels into noisy, clean, edge and possibly-corrupted classes. These discrete classes of pixels are treated differently. In case a pixel is identified as corrupted, the median filter is used and if the pixel is declared as possibly-corrupted, the degree of corruptness and possibly edginess is computed using fuzzy membership function and the weights are used to calculate the restored value; otherwise, the pixel is left unchanged.

  A spatially adaptive approach for selecting an appropriate threshold is presented that handles a huge diversity of real-world images except training or static (fixed) set up. The threshold parameters are set adaptively by exploring the adjoining pixels in 4-directions (horizontal, vertical and 2 diagonals) present in the neighbor of an impulsive pixel. The proposed technique is found to be robust to different noise densities (levels) and type of images (medical, natural, etc.), with a strong denoising capability.
- In **chapter 4**, a novel filter is proposed that uses local statistics based information (LLMMSE estimator) for uncertainty modeling based on a computational model – Fuzzy Uncertainty Modelling (FUM) for despeckling ultrasound images.

  The proposed fuzzy logic-based computational model gives superior performance both in terms of image despeckling and fine detail preservation.
  The proposed model is computationally efficient due to less number of multiplication and addition operations as only similar non-local regions of the image will be used to estimate the restored value of a noisy pixel. Proposed techniques detect and filter out noises without any training and an increase in computational complexity.

  Quantitative and qualitative analysis (in terms of local and global error measures) of the proposed techniques in this thesis prove their efficacy over the existing benchmarked restoration techniques.

1.8 Image Dataset

The performance of the proposed *"impulse*" and *"speckle*" noise filtering techniques have been evaluated both quantitatively and qualitatively by performing extensive experimentation on a large set of images (around 250 grayscale images) taken from well-known databases, USGS-Images and MedPix available at *www.imageprocessingplace.com*. The performance of the proposed despeckling technique is also assessed using experimentation performed on the synthesized, B-mode [40] ultrasonic simulated, Field-II [41] kidney simulated images. Experiments are also performed on real images of the liver and urinary tract taken from *www.ultrasoundcases.info*. All these experiments have been performed on a system having *"8 GB RAM and Intel Core i7 processor with 2.70 GHz clock speed"*. The prototype has been implemented in MATLAB 2015b (by The Math Works Inc.) in Windows 10 platform.

1.9 Image Performance Measures

The performance of the proposed filter is evaluated both subjectively as well as objectively.

1.9.1 Objective Image Quality Measure

The objective performance is measured using three widely used performance metrics, the *"Signal-to-Noise-Ratio"*, *"Peak-Signal-to-Noise-Ratio"* [42] which aims to measure the *"differences and similarities"* between the original noise-free image and the reconstructed image, "*Structure Similarity Index Measure"* [43] which is used to focus on the detail preservation characteristic and a novel low-level feature-based image quality assessment metric called *"Feature Similarity Index Measure"* [44]. FSIM measure relies on the fact that the *"Human Visual System"* recognizes an image mainly according to its *"low-level"* features.

These metrics are calculated as follows:

$$SNR(I_R, I_O) = 10\log_{10}\frac{\sum_{i=1}^{M}\sum_{j=1}^{N}(I_R)^2}{\sum_{i=1}^{M}\sum_{j=1}^{N}(I_O - I_R)^2} \quad (1.4)$$

$$PSNR(I_R, I_O) = 10\log_{10}\frac{I_{max}^2}{MSE(I_R, I_O)} \quad (1.5)$$

where,

$$MSE(I_R, I_O) = \frac{1}{M \times N}\sum_{i=1}^{M}\sum_{j=1}^{N}(I_R - I_O)^2 \quad (1.6)$$

$$SSIM = \frac{(2\mu_O\mu_R + C_1)(2\sigma_{OR} + C_2)}{(\mu_O^2+\mu_R^2 + C_1)(\sigma_O^2+\sigma_R^2 + C_2)} \quad (1.7)$$

$$FSIM = \frac{\sum_{x\in\Omega} S_L(x).PC_m(x)}{\sum_{x\in\Omega} PC_m(x)} \quad (1.8)$$

Here, I_O and I_R represent the original and reconstructed images respectively. I_{max} is the maximum pixel value in an 8-bit grayscale image which is 255, i and j represents pixel coordinates, $M \times N$ is the dimension of the image, μ_O and μ_R are the means, σ_O^2 and σ_R^2 are *"variances"* of the original and restored image respectively and σ_{OR} is the *"covariance"* of the original and restored image. PC_m denotes phase congruency and S_L is the similarity measure of the whole spatial image denoted by "Ω".

1.9.2 Subjective Image Quality Measure

Contrary to the above-listed performance measures, subjective image quality measure includes human perception for the assessment of restored images. It's a time-consuming process as different observers are asked to rate the restored image. It's a deterministic approach and may deviate from different observers.

1.10 Thesis Outline

After a brief introduction in Chapter 1, Chapter 2 presents a brief literature review and piles up the basic preliminaries of how IR techniques are formulated and solved. Chapter 3 presents a new quadrant based spatially adaptive filter that uses fuzzy inference and 4–directional background information to effectively restore the impulsive images. Chapter 4 proposes a novel speckle-noise reduction technique that uses Fuzzy Uncertainty Modelling (FUM) and non-local mean concept. Lastly, in Chapter 5, conclusions and future work directions are drawn.

Chapter 2

Review: Image Restoration Techniques

Chapter 2

2. Review: Image Restoration Methods

The prime objective of Image restoration is to recover or reconstruct an image when degraded by **noise** to produce a more accurate representation of the true image. The process of image restoration is objective in nature. Noise is usually termed as an unwanted variation in image data. Image analysis becomes simplified if the noise present in an image is filtered out. Scientists working in the Signal and Image Processing (SIP) domain have further elaborated the term *filter* to include actions that highlight features or structures of interest in signal and image data. In image processing, restoration techniques highlight different aspects to extract various important image features [2]. In this chapter, we briefly discuss basic mechanisms involved in image restoration and present a comprehensive literature review of related techniques to further elaborate the problem in hand.

2.1 Image Restoration Model

The main purpose of restoration is to 'undo' faults and defects which degrade the quality of an image. Degradation in images may occur due to motion blurring, presence of noise or camera defocus problem. In the case of motion blurring type of degradation, the original image can be restored by estimating the actual blurring effect and undoing the effect [42]. In noise corrupted images, the best thing we can do is to compensate for the degradation it caused. The image processing world has several techniques that can be used to restore images. Examples are spatial filtering, inverse filtering, Wiener filtering, wavelet restoration, etc.

For noise removal in spatial filtering, actions are carried out on the pixels of an image directly and most of the techniques in the literature review use this particular approach [45–51]. If we could estimate the model of degradation function accurately that corrupts the image, the inverse filtering concept can be used to restore the original

image. Unluckily, an inverse filter is a form of high pass filter which enhances the noise more, if present in the image. Inverse filtering can be used in the restoration techniques using thresholding or an iterative method. The block diagram of the image restoration model is presented in Fig. 2.1.

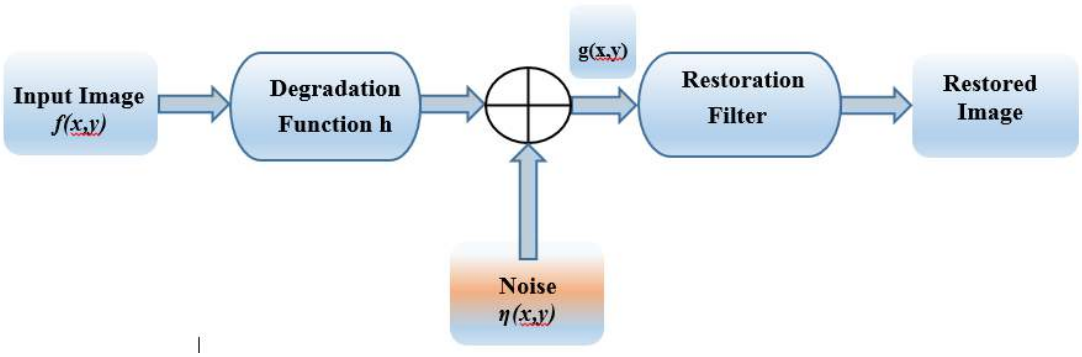

Fig 2.1: Image Restoration Model [2]

2.2 Image Filtering

Filtering is a technique that is used for enhancing and modifying an input image. When a specific filter is applied to an image, some of its features become prominent while others are wiped out. Edge enhancement, sharpening, and smoothing are common image processing operations employed with filtering. Filtering can be further divided into two types namely: spatial domain filtering and frequency domain filtering.

The term *spatial domain* denotes an aggregate of pixels composing an image. In this filtering mechanism, actions are directly carried out on pixels or elements of an image. The restored image is estimated using a restoration technique that works on neighboring pixels of the noisy input image. This estimation is accomplished via an operation called convolution [2].

In the *frequency domain*, an image of $n \times n$ elements is represented alternatively as a sum of *Sine waves* of different frequencies, directions, and amplitudes (also called *Fourier* representation). The parameters identifying the *sine waves* are labeled as *Fourier coefficients*. *Frequency domain filtering* is based on the conversion of the input image from the spatial to the frequency domain using Fast Fourier Transform (FFT), utilization of proposed filter, and conversion of the filtered image back to the spatial

domain using inverse Fourier Transform (IFT). Low pass, high pass and bandpass are the popular types of *frequency domain* filters [2]. In this research work, the proposed filters are mainly based on ***spatial domain filtering***.

2.2.1 Image Filtering in Spatial Domain

Spatial domain filtering is considered as an optimum option when additive noise is added to an image. In the spatial domain, different types of filters are used, which can be categorized into linear (mean), non-linear (order statistics), non-local[8] and adaptive filters [113]. Linear filters are widely used in IR algorithms in which the pixel values are replaced by the average value of its neighboring pixels. "*Harmonic filter, contra harmonic filter, arithmetic-mean filter and geometric-mean filter*" are the variations of the mean filter. These filters are good for IN removal but produce artificial artifacts by smearing the edges. Order statistics filters are good at detecting outliers in the processing window by exploiting simple sorting properties. Median filter, min-max filter, and midpoint filter are some of the examples of non-linear filters. Adaptive filters are considered most effective as filter behavior varies depending upon image contents [42].

2.3 Impulse Noise Model

As discussed earlier, impulse noise is of two types: fixed-valued and random-valued impulse noise. In fixed-valued impulse noise, a noisy pixel can take either a minimum 0 or a maximum 255 value from [0,255] interval in case of an 8-bit grayscale image. So the resulting image tainted with fixed valued impulse noise will have a black (for 0) or a white (for 255) spot on it. In the case of a random valued impulsive image, a pixel may become taint by taking any arbitrary value from the range [0−255]. Here the noise range is much broader than that of fixed valued impulse noise. Thus, the detection and restoration of random valued impulse noise from a deteriorated digital image are more common and more challenging than that of fixed valued impulse noise. Let $x_{r,c}$ and $y_{r,c}$ be the gray-level values at position (r, c) of the original and corrupted images respectively. Impulse noise for the grayscale image can be modeled as:

$$y_{r,c} = \begin{cases} \delta_{r,c} & with\ probability\ \rho \\ x_{r,c} & with\ probability\ (1-\rho) \end{cases} \quad (2.1)$$

where ρ is the probability that the pixel gets the noisy value and $\delta_{r,c}$ is the noisy pixel value coming from an Independent and Identically Distributed (IID) random process [52].

2.4 Related Work (Impulse Noise Reduction Techniques)

Linear filters, non-linear filters, and their variants have been exploited in state-of-the-art techniques to address different types of noises. These techniques present good results by performing the filtering process but may produce artificial artifacts and make the restored blurred images due to the fact that noisy and noiseless pixels are considered equally in the restoration process. Ordered statistical filters are non-linear in nature and are considered robust and effective against noise due to their restoration ability based on statistical measures and computational power [2,53–55]. These techniques compute the estimated restored value of a corrupted pixel by calculating the median of its neighboring directional pixels in a processing window. It does not produce the blurring effect but may spread the line or edge information in the image's detailed area. To overcome this limitation, a large number of median variants have been proposed in [33, 52,56–64] and are used especially for impulsive noise removal along with preserving the details to a great extent. In the following, some of the related techniques are reviewed that provides the base of the proposed filter.

2.4.1 Linear and Non-Linear Filters

T. C. Lin proposed an Adaptive CWM filter [65] which uses an adaptive operator that makes estimates by exploring the absolute difference between current/center pixel and the output of CWM [66] filter with different weights on the center, to detect the presence of impulsive noise. "Even though the filter gives some good results in terms of noise suppression but spoiling of noise-free pixels is more and it results in overall poor performance".

Tao Chen et.al [67] proposed a non-linear Multi-State Median filter that incorporates median and CWM filter into the noise detection phase to decide whether

the pixel under consideration is noisy or noiseless. The restoration phase is then applied to the pixel detected as noisy only. This filter suppresses the impulse noise present in the image while retaining the image detail to a great extent. "TSM filter provides steady performance when a specific range of threshold is applied".

Crnojevic et al. [68] introduced an efficient and effective local variance estimator (image detail), a modified version of MAD, which detaches the image details from the noisy pixels very efficiently. The iterative variant of MAD, Pixel-Wise MAD eradicates randomly distributed impulse noise present in the image. To separate image details from impulsive pixels, the “median of the absolute deviations from the median of MAD” is calculated and used. This filter eliminates all types of impulse noise efficaciously. The performance of the filter is above average but shows a decreasing tendency when the amount of texture/edge density increases.

Garnett et al. [69] presented ROAD, a new local image statistic to detect impulsive pixels. It is combined with a filter designed to remove mixed Gaussian and impulse noise.

DWM [33] filter introduced by Dong et al. proposed a new impulse detector which tends to amplify the differences between noise-free and noisy pixels by finding differences between the central and the adjoining pixels in the 4-directions (vertical, horizontal and two diagonal directions). A sliding window of size 5×5 is used to calculate the sum of absolute differences in the four directions. The minimum of these absolute difference values is compared with the threshold which marks the pixel as noisy or noise-free. In the filtering step, the direction of the line or edge, if exists, is determined by calculating the standard deviation in the above mentioned four directions. The value of the noisy pixel is replaced with the weighted median value calculated in the direction in which the standard deviation is small. This method yields good results when noise density is low but as the noise density increase, its performance gradually decreases.

An improved version of ROAD called ROD-ROAD is proposed by Liu et al. [70] which uses two-phase detection of an impulsive pixel with high accuracy and restores the value of noisy pixel using the weighted mean filter. The static threshold

value restricts the algorithm to be used only with a specific type of image and cannot be used generically.

Dawood et al. [62] proposed a filter that uses local statistics to identify the impulsive pixel. For this, the mean of the minimum of eight values of the absolute differences between the central pixel of a 5×5 processing window and all of its neighboring pixels are computed. Which is then compared with a static threshold value to classify the pixel as noisy or noise-free. In the filtering phase, a noisy-pixel is replaced with the median of the minimum difference pixels in optimal directions. The static threshold is the major problem that decreases the efficiency of the proposed filter.

Khan et al. [71] introduced an Adaptive Dynamically Weighted Median (ADWM) filter based on the CWM filter, in which weights of the central pixels are set dynamically. The proposed technique also uses an adaptive method that sets the processing rectangular window by increasing or decreasing the size according to the amount of impulsive noise.

Z Shi et al. [47] proposed an iterative two-phase noise filtering process based on an impulse detector that uses dissimilar pixel counting to deal with the mixture of Gaussian and impulse type of noise present in an image. The average difference between the neighboring pixels is used to find similarity or dissimilarity between the noisy and noise-free pixels. The total count of dissimilar pixels is compared with a static threshold to locate the outliers present in a noisy image. In the filtering phase, an extended trilateral filter is used to restore the value of noisy pixels. Proposed filter filter-out the mixed noise considerably while retaining the texture of the image intact to a large extent, but fails when noise density increases.

2.4.2 Fuzzy Logic based Restoration Techniques

A large number of image processing problems have been addressed by using fuzzy logic-based techniques. In image restoration, fuzzy logic has been used to remove fixed-valued and random-valued impulsive noise, eliminating Gaussian noise, at the same time preserving fine textured details and edges effectively. Linear filter theory is an effective tool to remove additive Gaussian noise but fails for non-additive Gaussian noise. In this connection, fuzzy logic-based methodologies for impulse and speckle noise reduction [46] have received attention because of reduced computational cost and

improved or almost akin restoration ability when they are compared with other bench-mark techniques. In the following, some well-known state-of-the-art fuzzy filters are reviewed in detail.

Histogram-based Fuzzy Filter has been proposed by Wang et al. in [72], a novel approach that exploits the image statistics (histogram) to estimate and suppress highly degraded impulsive images. HFF is a simple filter with low cost that gives better performance at medium noise densities but tends to perform poorly as the noise density increases especially in the textured area of the noisy image.

Schulte et al. proposed the Fuzzy Impulse Noise Detection and Reduction Method [73] in which a non-linear filter with fuzzy logic is used to eliminate both impulse and other mixture of noise with reduced time complexity. In the noise detection phase, a fuzzy rule-based system and different types of fuzzy membership functions are used to assess every pixel for noise or noise-free. In the noise reduction phase, only the detected noisy pixels are restored using fuzzy logic. Consequently, the image details (edges and textures) and the contrast remains unchanged. "This filter has the ability to reduce all kinds of impulse noises with a very low execution time".

Kang et al. proposed a Fuzzy Reasoning based Directional Median filter in [56] to overcome the problem with DWM filter [33] that states that the capability of the noise removal process reduces if edge directions are not identified by the DWM correctly. The difference between the current pixel and the 4-directional neighbors (edges) is calculated and used with the fuzzy logic to decide whether the current pixel is noisy, edge or noise-free. In noise filtering phase, a directional median filter is applied to restore the value of the noisy pixels. This filter filter-out the impulse noise considerably while preserving the details of the image to a large extent, but fails when noise density increases.

Wanga et al. [74] proposed Adaptive Neural Fuzzy Inference System, a novel impulse noise removal filter with a double noise detector scheme. In the detection phase, noisy pixels identified by the noise detector using an adaptive median filter are again judged by a local fuzzy membership function to improve the detection accuracy. In the filtering phase, noisy pixels are recovered using ANFIS based on the neighborhood of noise-free pixels.

In [51,52,57], an adaptive approach for threshold selection using fuzzy rules is proposed which efficiently utilizes the background pixel information to detect and deal with pixels tainted with specifically random valued impulse noise. The algorithm shows excellent results than the state-of-the-art filters in terms of qualitative and quantitative measures, detail preservation and noise suppression.

Schuster et al. [49] introduced a novel filter that first applies a simple median filter to reduce the impulsive noise followed by the application of direct fuzzy transform to the output image. Fuzzy rule-based logic is used to detect the noisy pixel and finally, its value is restored by applying an iterative impulse noise reduction method called AFT-IF. The proposed filter preserves the fine details present in the image while reducing the amount of impulse noise.

Roy et al. [63] introduced a region adaptive fuzzy filter for elimination of random-valued impulse noise from color images which take into consideration the correlation among the three color channels and recursively adapts itself to determine the maximum size of the rectangular window consistent with the local noise densities to detect and restore noisy pixels. The proposed filter preserves image detail considerably when noise density is low. As the noise density in the image increase, the performance of the filter starts decreasing.

A Roy et al. [45] presented a new impulsive filter that combines fuzzy c-means clustering and fuzzy support vector machine that removes impulse noise from color images. This method uses the Local Binary Pattern and the absolute difference between the median and the current pixel to detect noisy pixels. The fuzzy rule-based adaptive median filter is applied to restore the value of noisy pixels. The performance of the proposed filter gives good results in removing impulse noise considerably but tends to decrease when the noise density increases in the images.

During the last two decades, a significant number of research articles have been published in the field of image processing especially in the restoration of impulse noise from the degraded images using fuzzy logic. Recent techniques are much better than previous in all respect but no one can convincingly claim to have solved the image restoration problems completely.

2.4.3 Other Soft Computing & Vector-Based Techniques for Grey and Color images

EA based techniques are discussed in section 1.3.3 in detail. Genetic programming, evolutionary strategies (ESs), fuzzy-similarity and evolutionary programming (EP) are the basic types of EA. The difference between these methodologies comes in the way that how *search strategies* are implemented in each method.

Nemanja et al. [60] introduced an impulse noise filter based on the switching scheme that uses GP and local noise estimators, median and MAD. The technique is having the capability to suppress both salt & pepper and random-valued impulse noise. The GP based technique gives good results with exceeded computational time complexity.

Majid et al. [75] proposed an iterative impulse noise reduction scheme that starts working on a small number of noise-free pixels in a small size processing window and continues until all noisy pixels are restored using GP based noise estimator. Results produced by the technique are satisfactory with the capability to retain the fine details present in the image when the noise density is low.

SG Javed [76] presented an INDE-GP filter, a soft computing based noise removal technique that can deal with all kinds of impulse noise. First, IN is localized using GP combined with "*rank-ordered*" and robust "*statistical features*". Then only the detected impulsive pixels are restored using GP and local statistical measures of noise-free pixels present in the neighborhood of noisy pixels. The performance of the proposed filtering method in preserving the edges and texture slowly decreases as the noise ratio increases in the image.

To handle false artifacts produced by the noise in the images, vector-based non-linear gray and color image restoration techniques are introduced, which are based on robust local statistics [54,55] that perform ordering of vectors in a rectangular processing window [77] of some specific size. The fundamental tenet behind vector-based techniques is to *"rank the vectors with the help of an appropriate similarity measure"* using the reduced ordering principle. The vectors that are closest to other vectors in the window, based on a distance measure, are considered as the lowest-

ranked vectors. So, noise can be detected very easily by looking at the highest-ranked vectors in the processing window.

The main limitation of the vector-based color filters is that they cannot adapt to images with different levels of details because of a fixed amount of filtering. Therefore several modified versions of vector filters are developed. Schulte et al. [78] proposed HFC filter for image restoration. This filter tries to maintain color differences while using a well-known HFF [72] algorithm for color images and therefore outperforms other techniques for color image restoration. This technique uses only a single fuzzy membership function. Other fuzzy membership functions have not been explored.

From the above literature review, it is clear that removal of random-valued-impulse-noise is more challenging than fixed-value-impulse-noise and such noise is more likely to come in real-world applications. It is further noted that the noise removal techniques are heavily dependent on noise detection mechanism. Therefore, the accuracy and estimation power of the noise detector is a very important factor in the noise removal process. More work is required in grey as well as colored image restoration as most of the filtering techniques have problems at high noise densities, distortion, and generating false artifacts.

2.5 Speckle Noise Model

Mathematical model of the speckle noise given in Eq. 2.2 shows that the noise distribution in ultrasound medical image is signal-dependent and multiplicative in nature [1] and is given as under:

$$I^{noisy}(x) \approx I^{original}(x)\eta(x) \tag{2.2}$$

The original image is represented by $I^{original}(x)$, x is the pixel location, the observed image with noise is represented by $I^{noisy}(x)$ and $\eta(x)$ specifies the multiplicative noise component. The following equation is obtained after applying log transformation to the mathematical model given in Eq. 2.2.

$$\log\left(I^{noisy}(x)\right) \approx \log\left(I^{original}(x)\right) + \log\left(\eta(x)\right) \tag{2.3}$$

The general model of the speckle-noise present in almost every ultrasound image is given in the following expression:

$$I^{noisy}(x) = I^{original}(x) + I^{original}(x)^{r} * \eta(x) \quad (2.4)$$

where factor ***r*** is attributed to the ultrasound acquisition device having Gaussian distribution with zero mean. In the ultrasound image study of B-mode, a good representation of ultrasound data is made by setting ***r*** equal to 0.5. The model shows that speckle noise is multiplicative when ***r*** is set to 1.

2.6 Related Work (Speckle Noise Reduction Techniques)

Unlike other non-invasive imaging techniques, ultrasound images are playing a vital role in medical diagnostics to visualize and examine the internal human body structures due to its portability, substantially cost-effective nature and harmless ionizing radiations. During the acquisition or transmission process, these images may corrupt by additive and multiplicative speckle noise [2,7]. Speckle is a granular noise that inherently degrades the quality of the image resulting in complications for the detection of small edges and other textural details.

Image denoising is a required pre-processing step for every image processing and computer vision task. It helps in extracting reliable and accurate information using segmentation, feature extraction and classification purposes from the ultrasound image. The current study addresses the multiplicative type of uncertainty present in almost every ultrasound medical image.

The speckle in the US image is often considered as undesirable and numerous noise removal techniques have been proposed considering the signal-dependent nature of the speckle intensity. In the next section, a comprehensive review of standard adaptive filters and other methods for speckle reduction is presented.

2.6.1 Standard Adaptive Techniques

Medical image smoothing may cause the blurring effect while edge sharpening may lead to noise amplification [79]. In most of the existing denoising methods, filtering is performed on the whole image rather than applied to the noisy part of the

image only. As a result, noise-free pixels also get change which destroys the image content considerably and produces false artifacts. In order to despeckle the images considerably, specific filters have been designed both in spatial and transformed domains [80]. Existing methods use a variety of adaptive local statistical spatial filters such as average, median, wiener, Lee, Frost, and Kuan filters [81–83]. These filters provide a visually enhanced image to make an accurate diagnosis by reducing speckle noise effectively, but quantitative analysis shows that they do not precisely preserve the important features of the required data such as thin lines, edges and anatomical boundaries in the image.

2.6.2 Partial Differential Equations (PDE) based Methods

A balance between the preservation of useful diagnostic information and noise suppression is the main goal of CAD. To preserve the fine edges and suppress speckle in images, Anisotropic Diffusion filter [38] and its variants Speckle Reducing AD filter [84], Oriented SRAD filter [85] are used. These filters work well for regional features preservation but for point and linear feature characterization, they need to be corrected. Due to the iterative nature of these filters, some important detail may disappear from the image which is the major drawback of this technique. To preserve the minor details, the Squeeze Box filter [86] is proposed as a preprocessing step for enhancing the contrast of B-mode images by compressing the pixel distribution range to some limit in homogeneous regions while preserving the average mean values of distinct regions of the image by using local statistical functions. To address the speckle noise in the image, other transform domain denoising methods are also used. However, almost all methods generally produce unwanted or false artifacts in the image which can lead to false diagnoses. So more robust and accurate detail preserving despeckling filters are in need and being sought. The despeckling methods mentioned above are based on local statistical information. The pixels in the image are highly correlated and the noise is generally independent, so to simply averaging these pixels yield considerable noise reduction, but makes the edges more blurred.

2.6.3 Switching Scheme based Methods

A "*Switching scheme concept*" is introduced in [50] that improves the speckle noise detection process without affecting the image details. This technique identifies

the deteriorated pixels from the noisy image first, then only these pixels are subjected to the noise removal process leaving the noise-free pixels unchanged. Most of the newly proposed filtering techniques are now use this switching scheme for restoration.

2.6.4 Deep Learning-based Methods

Over recent years, DL [87,88] has had a remarkable impact on various fields in science. It has led to substantial improvements in image restoration, image segmentation, image detection and recognition, image registration and speech recognition. This technology is also highly relevant for medical imaging. There have been several attempts to handle the denoising problem by DL algorithms [89–91]. Despite the promising results, DL-approach has some shortcomings as well. One of the biggest hurdles of DL research in medical imaging is the data-hungry nature of the DL algorithms. It needs to be trained with large sets of labelled data. The larger the training data set, the better the performance of the algorithm. Secondly, it is computationally very expensive which restricts it to be used in a real-time scenario. Furthermore, a DL algorithm requires many tuning parameters to properly train the model that makes it difficult to configure. The complexity of the hidden layers of the DL algorithm hinders to interpret the results or to understand the algorithm mechanism.

2.6.5 Non-Local Mean based Methods

Non-Local Mean filtering [8,92] is a non-local technique in which only selected regions are used to model the uncertainty present in the image. NLM analyzes the data in large and collects the observations from the whole image looking for similar features. This technique removes the noise cleanly preserving the edges and other fine details. This filter uses similar local regions within the image to calculate the weights of the pixels contain noise. NLM filter is best to restore a periodic or textured image. Due to this property, the NLM filter has proven to be an effective and efficient restoration technique and has been used by many researchers to despeckle ultrasound images. OBNLM (Optimized Bayesian NLM) [93] filter uses a Bayesian framework is also adopted to address speckle noise. The performance of the NLM filters is inversely related to the degree of noise in the image. As the noise increase, the NLM and its variants start to produce blurring effects within the image which decreases its quality. Therefore, NLMLS (Non-local mean filter combined with local statistics) [39] is

proposed that combines the best features of local statistics and NLM filter and effectively reduce the speckle noise in the ultrasound images. The noisy regions input to the NLM, are first smoothed based on the local statistical features which are then used to compute the weights for the NLM. Results show significant improvement in the quality of the despeckled ultrasound image. Another hybrid algorithm for making noise-free ultrasonic images [41] uses a three-step non-iterative process to despeckle the ultrasound images. The local statistical information of the image is obtained and is used to reduce speckle noise in the first step followed by applying improved SRBF – "*Speckle Reducing Bilateral Filter*" to further lessen the speckle noise. In the third step, the NLM filter is applied to reconstruct the diffused edges as a post-processing technique.

2.6.6 NLM based Fuzzy Mechanism

NLM filters using a fuzzy similarity mechanism have also been proposed recently for eliminating random valued impulse noise, multiplicative speckle noise and rician noise from the medical images [94–96]. These methods use fuzzy logic to identify the degree of similarity between multiple non-local regions present around the noisy pixel.

2.7 Summary

In this chapter, basic preliminaries of image filtering and common methods for addressing IR problems have been conferred. Noise filtering algorithms are primarily reliant on noise detection mechanism in which optimization, accuracy and estimation power of noise detector is very important. Most of the existing IN and Speckle noise filtering algorithms (linear, non-linear, directional, non-directional, NLM and other soft computing based techniques) use fixed threshold parameters and do not make full use of the processing window which ultimately reduce the noise detection as well as edge preservation capabilities. To address these problems, a fuzzy inference system based adaptive mechanisms have been proposed in this thesis for effective cancellation of noise and preservation of edge s and other fine detailed information.

Chapter 3

Quadrant based Spatially Adaptive Fuzzy Filter for Random Valued Impulse Noise Removal

Chapter 3

3. Quadrant based Spatially Adaptive Fuzzy Filter for Random Valued Impulse Noise Removal

In this chapter, an efficient image restoration technique Quadrant based Spatially Adaptive Fuzzy filter [97] is presented which is based on spatially linked-directional adjoining pixels and fuzzy logic for addressing moderate and highly corrupted grayscale images with Random Valued Impulse Noise is presented. The proposed technique decomposes a larger sized impulsive region of an image into numerous overlapping small patches for low as well as high-density impulse noise estimation with enhanced image restoration results. This subdivision highlights the details (edges, lines, and textures) present in the neighborhood and the locations of impulsive pixels are relocated in multiple regions. Direction-based fuzzy rules give appropriate reasoning for edge and texture detection in an image. A switching technique based fuzzified degree identifies a certain pixel of an image as a noise-free, noisy or edge pixel in the filtering phase. Instead of using a static threshold, a directional non-parametric approach is introduced that determines and sets the threshold adaptively which empowers the proposed filter to handle different types of images automatically.

3.1 Motivations

As discussed earlier in chapter 2, the impulsive noise has a characteristic that it swaps only a random subset of the clean image pixels with impulse noise leaving all other pixel values unchanged. Many existing impulse noise restoration techniques tend to fail when the following three cases are considered:

Case–1:

Filtering techniques based on mean [70,98,99] and median [30–37,68,69,100–104] operations fail to approximate the actual value of an impulsive pixel if half or more of the processing window is affected with impulse noise. Fig. 3.1(a) shows a *3×3* noise-free window. A smooth region tainted with *Salt-impulse* and *Pepper-impulse* is shown in Fig. 3.1 (b) and (c) respectively. The mean filter fails to restore the central pixel value accurately as in Fig. 3.1(b) the restored value will be 171 and in Fig. 3.1(c) it will be 29. Whereas median filters recognize the central pixel as noise-free in both cases as the difference (absolute) between the median of neighbor and center pixel is zero.

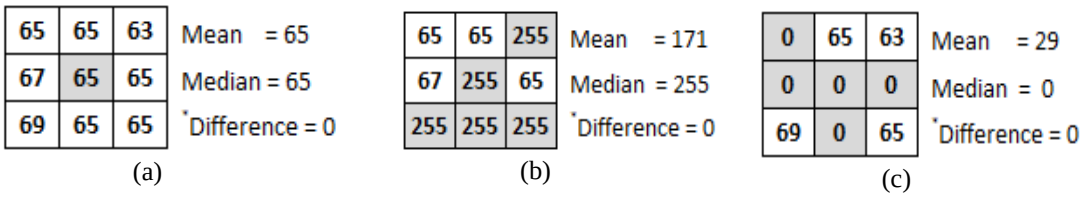

Fig. 3.1: (Case–1) (a) *3×3* noise-free window (b) Salt and (c) Pepper Impulse noise in the smooth region representing Mean, Median and *Difference (between the central pixel and median of the window)

Case–2:

In the case of fine-textured and detailed images corrupted with RVIN, the absolute difference between pixels in a region is larger than normal. As a result, it is very difficult to distinguish between a fine-textured pixel value and a random noise value. Fig. 3.2 (a) and (b) show a processing window of size *3×3* tainted with RVIN and a free from noise respectively. The difference (absolute) between the median of neighboring pixels and the central pixel of both windows are 38 and 37, respectively. As the differences are very close, so it is difficult to separate noise from fine-textured patches. Techniques presented in [56,73,105,106] are unable to identify noisy pixels precisely in this case.

Case–3:

Fig. 3.2(c) shows another problem when the central pixel of a uniformly distributed patch of the image is affected with RVIN and the difference between the central pixel and median is very small. Most of the state-of-the-art methods [51,57,58]

perform quite well in the case of large outliers but become inefficient against small variations.

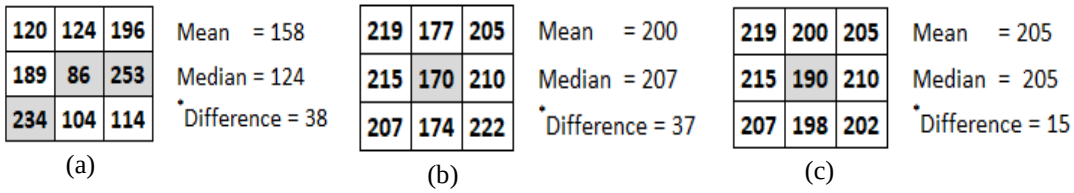

Fig. 3.2: (Case–2) (a) *3×3* window affected with RVIN (b) noise-free window (c) Central pixel affected with RVIN representing Mean, Median and *Difference (between central pixel and median of the window)

A novel, robust and detail-preserving filter has been proposed in this research that tackles any type of impulsive noise present in the image. The proposed iterative filter sub-divides a large-size processing window into numerous smaller overlapping windows to form a *quadrant set*. A *quadrant vector* is computed from the sorted estimated *medians* of the small-size windows. This *quadrant vector* uses fuzzy rule-based reasoning to further explore the presence of impulse noise and the amount of texture in an image. In the restoration process, a simple switching median technique is used to restore the value of the impulsive pixel. The proposed technique successively detects and suppresses low, medium and high-density impulse noise from the deteriorated images while preserving the fine structure and details on a large scale. Experiments show that the proposed technique is equally effective for both the RVIN and SPN.

3.2 Contributions

Major contributions made in this chapter are as follows:

- A robust switching scheme based on fuzzy logic and statistical parameter estimation is proposed that uses the divide and conquer strategy to deal with low as well as a high degree of impulse noise present in the image.
- Fuzzy rules are exercised to categorize the impulsive pixels into noisy, clean, edge and possibly-corrupted classes.
- These discrete classes of pixels are treated differently. In case a pixel is identified as corrupted, the median filter is used and if the pixel is declared as possibly-

corrupted, the degree of corruptness and possibly edginess is computed using fuzzy membership function and the weights are used to calculate the restored value; otherwise, the pixel is left unchanged.

- A spatially adaptive approach for selecting an appropriate threshold is presented that can handle a huge diversity of real-world images except training or static (fixed) set up. The threshold parameters are set adaptively by exploring the adjoining pixels in 4-directions (horizontal, vertical and 2 diagonals) present in the neighbor of an impulsive pixel.
- The proposed technique is found to be robust to different noise densities (levels) and type of images (medical, natural, etc.), with a strong denoising capability. Experiments show that the denoising results obtained by the proposed method outperform its counterparts at low, medium and high noise densities.

3.3 Proposed Filter

To address the limitations of the existing methods discussed in chapter 2, in a case when more than 50% of the pixels in the selected processing window are affected with impulse noise and to remove low as well as highly corrupted pixels, we have introduced a new methodology in which a processing window of size $n \times n$ is subdivided into an overlapped set of sub-windows of reduced size where the fuzzy rule-based system is used to deal with the uncertainties present in the image as shown in Fig. 3.3.

The proposed filtering technique is based on an adaptive switching mechanism that detects the noisy pixels in the degraded image and restores those pixels by using a fuzzy rule-based directional median operation leaving noiseless pixels unaltered.

3.3.1 Impulse Noise Detector

In the noise-free image, the neighboring pixels show high cohesion with each other i.e. slow varying intensity values in case of smooth regions and high varying intensities in different directions in case of lines or edges. Whereas in impulsive images, due to the unexpected random change in the intensity values, noisy pixels lose coupling with their neighbors and the fine structure is lost.

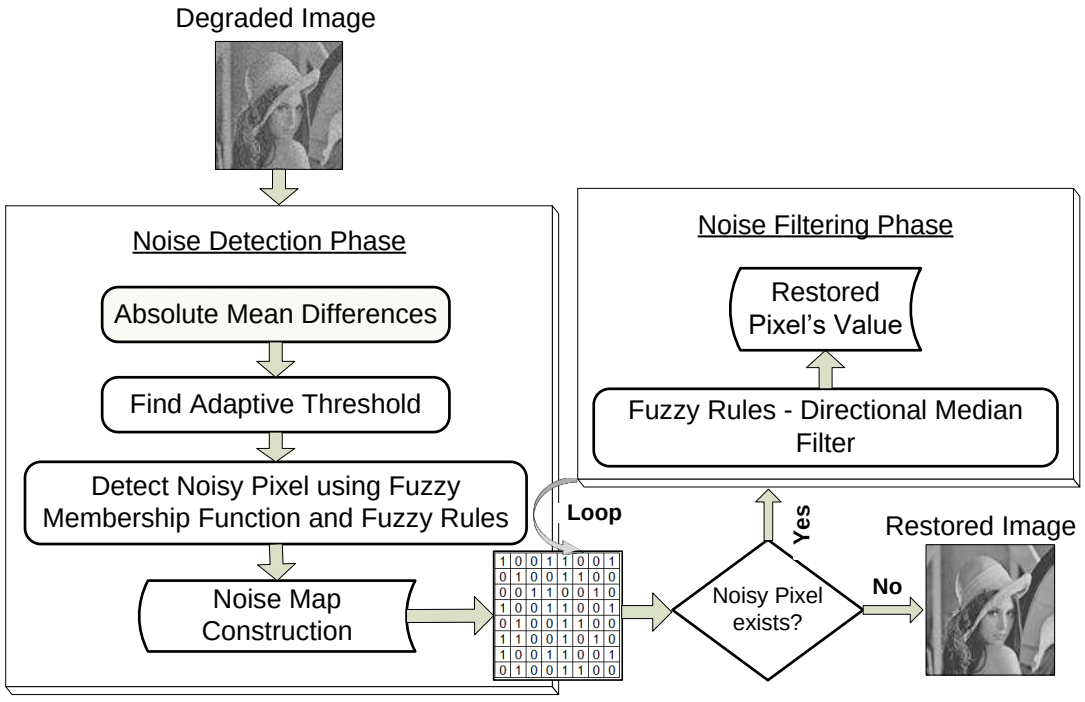

Fig. 3.3: Block diagram of the proposed RVIN filter

Impulsive pixels can be identified through the analysis of local statistical properties of a small patch of the degraded image (processing window), whose size is bounded by the filter. Selecting the appropriate size of the processing window is very critical and should be given due consideration in any impulse noise detector algorithm. More information regarding fine details like edges and textures are obtainable in processing windows having a large size, whereas small size processing windows are robust to the detection of small scale noise densities.

Let ω be a square $(2n+1) \times (2n+1)$ processing window. A mixed approach has been introduced that uses two processing (sliding) windows of different size represented by ω^n, where $n = 1,2$ taking into consideration the *"median drifting"* problem in processing window of size *5×5* and *"lack of texture"* issue in a very small processing window of size *3×3*. To achieve this aim, a processing window of size ω^2 i.e., *5×5* is apportioned into several overlapped sub-windows (*quadrants*) of size ω^1 i.e., *3×3* each. An illustration is shown in Fig. 3.4.

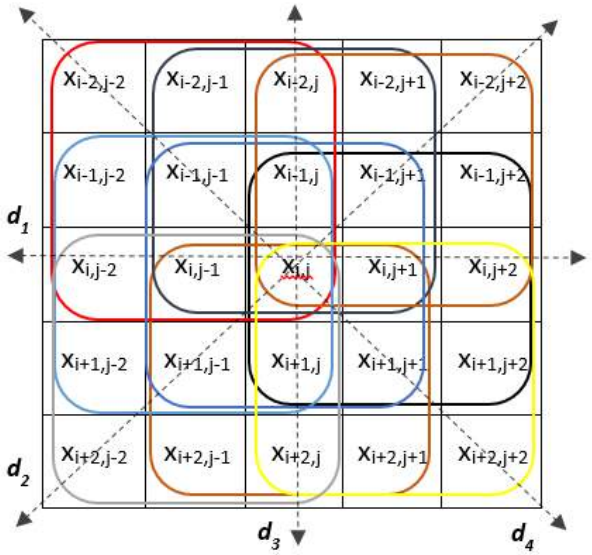

Fig. 3.4: A *5×5* window is divided into *3×3* overlapped sub-windows (*Quadrants*), d_1,d_2,d_3,d_4 represents four directions

This subdivision has a special benefit that a pixel degraded with an impulse noise at the central position in a processing window ω^2 remains no more at that position in a processing window ω^1.

3.3.2 Quadrant Set and Quadrant Median Vector

Let $x(.,.)$ denotes a discrete image sequence with noisy pixels centered at a location (i,j) in a processing window $\omega^n = \{(s,t)| -n \le s \le n, -n \le t \le n\}$, where $n = 2$ and let $q_l^{\omega^1}, l = 1,2,\dots,9$, be the nine quadrants of size *3×3* each. The location of the pixels in nine quadrant sets are defined as:

$$q_1^{\omega^1} = \{x(i+s, j+t): -2 \le s \le 0, -2 \le t \le 0\} \quad (3.1a)$$

$$q_2^{\omega^1} = \{x(i+s, j+t): -1 \le s \le 1, -2 \le t \le 0\} \quad (3.1\ b)$$

$$q_3^{\omega^1} = \{x(i+s, j+t): \ \ 0 \le s \le 2, -2 \le t \le 0\} \quad (3.1\ c)$$

$$q_4^{\omega^1} = \{x(i+s, j+t): -2 \le s \le 0, -1 \le t \le 1\} \quad (3.1\ d)$$

$$q_5^{\omega^1} = \{x(i+s, j+t): -1 \le s \le 1, -1 \le t \le 1\} \quad (3.1\ e)$$

$$q_6^{\omega^1} = \{x(i+s, j+t): \ \ 0 \le s \le 2, -1 \le t \le 1\} \quad (3.1\ f)$$

$$q_7^{\omega^1} = \{x(i+s, j+t): -2 \le s \le 0, \ \ 0 \le t \le 2\} \quad (3.1\ g)$$

$$q_8^{\omega^1} = \{x(i+s, j+t): -1 \le s \le 1, \ \ 0 \le t \le 2\} \quad (3.1\ h)$$

$$q_9^{\omega^1} = \{x(i+s, j+t): \ \ 0 \le s \le 2, \ \ 0 \le t \le 2\} \quad (3.1\ i)$$

Each sub-neighborhood or set $q_l^{\omega^1}, l = 1,2,\ldots,9$ has estimated median values and are defined as follows:

$$v_l = MED\{q_l^{\omega^1}\}, l = 1,2,..,9 \quad (3.2)$$

where $MED()$ is a median filtering operation and $v_1, \ _2, \ldots, v_9$ are estimated medians of nine sub-windows/quadrant-sets given in Eq. 3.2.

$$\vec{V} = [\overline{v_1}, \overline{v_2}, \overline{v_3}, \overline{v_4}, \overline{v_5}, \overline{v_6}, \overline{v_7}, \overline{v_8}, \overline{v_9}] \quad (3.3)$$

$$R_1 = Mean(\omega^n) - x(i,j) \quad (3.4)$$

$$R_2 = \sum_{i=2}^{9}(V_i - V_{i-1}) \quad (3.5)$$

These median values are put in ascending order such that $\overline{v_1}<\overline{v_2}<\overline{v_3}\ldots<\overline{v_9}$, where $\overline{v_1}$ and $\overline{v_9}$ are the smallest and largest estimated medians, respectively and forms a quadrant vector consisting of sorted estimated medians given in Eq. 3.3. R_1 shows the degree of central pixel deviation from the mean of the processing window given in (3.4). R_2 is the Rank Ordered Difference of the vector $\vec{V}$ given in Eq. 3.5. Higher the value of R_1 and R_2, greater is the chance of a pixel to be noisy. Here, R_1 and R_2 are used to decide whether the pixel under consideration is noisy or noiseless.

3.3.3 Fuzzy Rules and Fuzzy Member Function

Schulte et al. [73] used fuzzy logic to determine whether the pixel under consideration is impulsive or not by assigning the *degree of impulsiveness* to each pixel by using fuzzy gradient values. To differentiate noisy pixels from edge pixels, the difference between the gradients is calculated and checked whether it is *Large* or *Small*. Because *Large* and *Small* are non-deterministic features, these terms can be represented as fuzzy sets [107]. These fuzzy sets are represented by fuzzy membership functions *Small(x)* (for fuzzy set *Small*) and *Large(x)* (for fuzzy set *Large*) as shown in Fig. 3.5. Depending upon the nature of the data and the capability to distinguish noisy pixels from clean pixels effectively, trapezoidal-shaped fuzzy membership functions have been used [49,51,52,56,57].

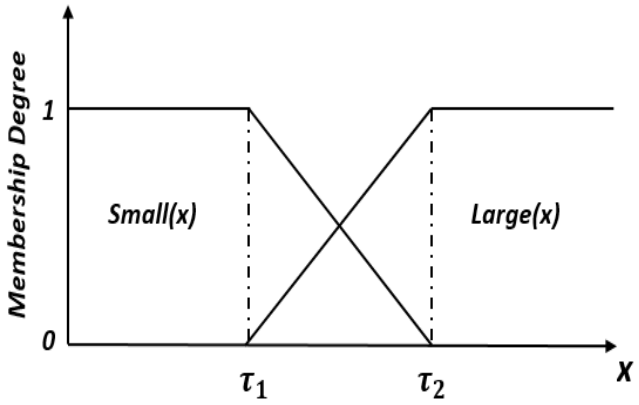

Fig. 3.5: Trapezoidal Fuzzy membership functions '***Small'*** and '***Large'***

To reduce the computational complexity of the fuzzy rule base by making it simpler, two inputs R_1 given in Eq. 3.4 and R_2 given in Eq. 3.5 have been used to fire four fuzzy rules. These are defined as:

$$r_1 = Small(R_1, \tau_1, \tau_2).Small(R_2, \tau_1, \tau_2) \quad (3.6\text{ a})$$

$$r_2 = Small(R_1, \tau_1, \tau_2).large(R_2, \tau_1, \tau_2) \quad (3.6\text{ b})$$

$$r_3 = large(R_1, \tau_1, \tau_2).Small(R_2, \tau_1, \tau_2) \quad (3.6\text{ c})$$

$$r_4 = large(R_1, \tau_1, \tau_2).large(R_2, \tau_1, \tau_2) \quad (3.6\text{ d})$$

The trapezoidal-shaped fuzzy membership functions *'Small'* and *'Large'* are intended as:

$$Small(R_1, \tau_1, \tau_2) = \begin{cases} 1, & R_1 < \tau_1 \\ \left(\dfrac{R_1 - \tau_2}{\tau_1 - \tau_2}\right), & \tau_1 \le R_1 < \tau_2 \\ 0, & R_1 \ge \tau_2 \end{cases} \quad (3.7)$$

$$Large(R_1, \tau_1, \tau_2) = \begin{cases} 0, & R_1 < \tau_1 \\ \left(\dfrac{R_1 - \tau_1}{\tau_2 - \tau_1}\right), & \tau_1 \le R_1 < \tau_2 \\ 1, & R_1 \ge \tau_2 \end{cases} \quad (3.8)$$

where τ_1 and τ_2 are threshold parameters and are discussed in the next section.

After firing all fuzzy rules, fuzzy *"membership degree"* is determined as:

$$\mu_{degree} = MAX(r_1, r_2, r_3, r_4) \tag{3.9}$$

3.3.4 Adaptive Threshold setting via Directional Non-Parametric approach

The limitation of existing impulse noise removal filters is that they require either static or ad-hoc threshold [58,69]. This limits the denoising algorithm to be used only for a specific type of image and also increases the computational cost in case of complex techniques that require training procedures. In response, we have introduced an adaptive threshold setting approach that is independent of the training process or static parameter setting. For a given impulsive pixel $x(i,j)$, the threshold value is determined adaptively from the local area (neighboring pixels) spanned by the processing window. In this technique, a processing window $\omega^n = \{(s,t)| -n \leq s \leq n, -n \leq t \leq n\}$, with $n = 2$ centered at $x(i,j)$ is used that computes the absolute luminous differences between $x(i,j)$ and its neighbors as:

$$g_d(i,j) = \frac{\sum_{v \in \omega^n{}_d} |v - x(i,j)|}{(2n+1)^2 - 9}, \quad d = 1,2,3,4 \tag{3.10}$$

where $'v'$ is the set of pixels in the processing window ω^2 in direction $'d'$ as shown in Fig. 3.4 excluding central pixel. To reduce the computational cost, only four directions mentioned in DWM [33] filter are considered. Image pixels degraded with random impulse noise will generally have large $g_d(i,j)$ values due to the fact that these pixels mostly occur as outliers in comparison to their neighborhood. This assumption becomes false in the following two cases:

- $g_d(.,.)$ will generate high value, in case one of the neighboring pixels is an impulse but the central pixel is noise-free.
- Naturally, $g_d(.,.)$ will have a large value for an edge in an image.

To treat these two cases, we have introduced two parameters φ_1 and φ_2 given in the following equations.

$$\varphi_1(i,j) = \frac{\sum_{s=-2}^{2}\sum_{t=-2}^{2} g_d(i+s, j+t)}{(2n+1)^2} \tag{3.11}$$

$$\varphi_2(i,j) = g_d(i,j) \tag{3.12}$$

A pixel $x(i,j)$ is treated as an *'edge'* pixel if φ_1 and φ_2 both have *Large* values, while a pixel is treated as *noise* if the difference between the values of φ_1 and $\varphi_2$is *Large*. This can be carried out by the fuzzy rule given below:

Fuzzy Rule: IF φ_1 is *Large* and φ_2 is *Large*

Then pixel $x(i,j)$ is an edge pixel

Else IF $|\varphi_1 - \varphi_2|$ is *Large*,

Then pixel $x(i,j)$ is an impulsive pixel

In this Fuzzy rule, as discussed earlier, *Large* is a fuzzy set, which is represented by fuzzy membership function *'Large'* and is extracted as:

$$\eta_{noise}(i,j) = \mu_{Large}[|\varphi_1(i,j) - \varphi_2(i,j)|,\ \tau_1(i,j), \tau_2(i,j)] \tag{3.13}$$

In a *"fuzzy set"*, membership degrees are the values that cover the whole range of [0,1]. Here the value '0' represents a noise-free pixel and noisy-pixel is represented by '1'. All other possible values of the membership degrees between the range 0 to 1 correspond to the degree of doubt (ambiguity) that whether the pixel is noise or an edge.

To eradicate this ambiguity, two new parameters τ_1 and τ_2 have been introduced given in Eq. 3.14 and Eq. 3.15. τ_1 corresponds to the $g_d(i+s, j+t)$ value computed from the most *"homogeneous"* region in the neighborhood of the pixel $x(i,j)$, which should conform to the region with the less number of impulsive pixels.

Experimental results in the literature have verified that the best option for parameter τ_2 is given in Eq. 3.15, i.e. larger the parameter τ_1, larger becomes the uncertainty interval $[\tau_1, \tau_2]$. The outputs of the detection method are the membership

degrees in the fuzzy set represent the impulse noise for each pixel separately, denoted by $\eta_{noise}(.,.)$.

$$\tau_1(i,j) = Min_{s,t\,\varepsilon\,\{-2,\ldots,+2\}}(g_d(i+s,j+t)) \quad (3.14)$$

$$\tau_2(i,j) = \tau_1(i,j) + [0.2 \times \tau_1(i,j)] \quad (3.15)$$

3.4 Impulse Noise Filtering method

The detection method is applied to determine the pixels that carry the noise element. The filtering method should be applied only to these leaving all other pixels unaltered. Membership degrees play a vital role in the filtering phase. Pixels with membership degree (μ_{degree}) = r_1 is treated as a noisy pixel, and is restored using median operation. Pixel with μ_{degree} = r_2 or r_3 is treated as noisy or edge pixel, and is filtered using a median-based fuzzy filter. Pixels with μ_{degree} = r_4 are considered as noise-free or edge pixels. Filtering rules are in the form of IF-Then-Else and given as:

IF ($\mu_{degree} = r_1$) **Then** **// (Noisy-Pixel)**

$F(x,y) = MED(\omega^n)$

Else IF ($\mu_{degree} = r_2$ or r_3) **Then** **// (Noise/Edge Pixel)**

$F(x,y) = \eta_{noise}(i,j) \times MED(\omega^n) + [1 - \eta_{noise}(i,j)] \times x(i,j)$

Else **// (Noise Free/Edge Pixel)**

$F(x,y) = x(i,j)$

3.5 Results and Discussion

To evaluate the performance of the proposed technique quantitatively and qualitatively, extensive experimentation has been performed on a large set of images (around 250 grayscale images) taken from well-known databases given in section 1.8. Each of the test images is degraded with the impulse noise model described in Eq. 2.1 having noise density ranging from 10% to 60% in step of 10% before subjecting to the proposed restoration process. The testing results of a set of images found frequently in the literature i.e., Lena, Pepper, Boat, Pentagon and Bridge of size *512×512* shown in Fig. 3.6 are presented in this chapter.

(a) (b) (c) (d) (e)

Fig. 3.6: Test images (*512×512*) (a) *Lena* (b) *Pepper* (c) *Boat* (d) *Pentagon* (e) *Bridge*

3.5.1 Parameter Setting

There are only two parameters that should be predetermined in the proposed technique. The first parameter is the number of iterations "*n*" that plays a key role in improving the detection rate and restoration capability. Its optimal value depends on the RVIN noise intensity present in the image. For a low and wide range of noise ratio, the optimal effect is achieved after the first and third iteration respectively.

The second parameter is the appropriate size of the processing window. We have chosen *5×5* size window which is again subdivided into nine overlapped sub-windows of size *3×3* (quadrants) keeping in view the median drifting problem in *5×5* and lack of texture problem in *3×3* sized windows as discussed in section 3.1.

3.5.2 Performance of Proposed Noise Detector

As discussed earlier, the performance of a good filter is directly dependent on the ability of a noise detector to detect noisy pixels accurately. In the case of RVIN, where the intensity value of the noisy pixel is not much different from its neighbors, the chances of missing the noisy pixel or detecting the noise-free as noisy by the impulse noise detector are very high.

A good noise detector should have the capability to detect noisy pixels accurately and also minimize the count of missing noisy or false detection of pixels. The comparison of accuracy of proposed noise detection mechanism with some of the well-known noise detectors for "*Lena"* image corrupted with 40% ~ 60% in step of 10% RVIN noise levels is presented in Table 3.1.

The table lists the number of truly detected noisy pixels ("*True Hit*"), undetected noisy pixels ("*Miss Hit*"), falsely detected as noisy pixels ("*False Hit*") and the accuracy (%) of truly detected noisy pixels by the various methods. From Table 3.1, it can be seen that the proposed noise detector has the best *"True Hit"* accuracy as compared to other competitive noise detectors even in case of highly corrupted images.

Table 3.1: Comparison of Accuracy of the Detection Mechanism for "*Lena"* image corrupted with various RVIN noise levels

Methods	**40%** (Corrupted Pixels: 104,858)				**50%** (Corrupted Pixels: 131,072)				**60%** (Corrupted Pixels: 157,286)			
	True Hit	**Miss Hit**	**False Hit**	**True Hit Accuracy (%)**	**True Hit**	**Miss Hit**	**False Hit**	**True Hit Accuracy (%)**	**True Hit**	**Miss Hit**	**False Hit**	**True Hit Accuracy (%)**
SDOOD [101]	91589	13269	10324	87.35	119330	11742	15574	91.04	140297	16989	5923	89.20
DWM [33]	95350	9508	7734	90.93	121427	9645	11373	92.64	144610	12676	12351	91.94
ATFDF [108]	99224	5634	7895	94.63	123640	7432	8976	94.33	147897	9389	9012	94.03
ACWM [109]	88806	16052	**1759**	84.69	107389	23683	**3623**	81.93	124574	32712	**7644**	79.20
MDW [103]	99624	5234	8962	95.01	123505	7567	9342	94.23	**149274**	**8012**	9787	**94.91**
NWM [70]	94709	10149	5212	90.32	121956	9116	11299	93.05	141838	15448	7449	90.18
AFIDM [57]	99649	5209	7069	95.03	123965	7107	8374	94.58	147321	9965	8895	93.66
Proposed Method	**99854**	**5004**	6403	**95.23**	**124149**	**6923**	8023	**94.72**	**148731**	**8555**	9232	**94.56**

3.5.3 Performance of Proposed Filter

The performance of the proposed filter is evaluated both subjectively as well as objectively. The objective performance is measured using three widely used performance metrics, the Peak-Signal-to-Noise-Ratio (PSNR), Structure Similarity Index Measure (SSIM) and Feature Similarity Index Measure (FSIM) discussed in section 1.9.1.

For objective and subjective analysis, the performance of the proposed filter is compared with several benchmarked filter techniques such as DPC-INR[47], TF[69], NLM[92], DWM[33], ACWM [109], ATFDF[108], SBF[104], CEF[102], SDOOD[101], MDW[103], NWM[70] and AFIDM [57]. The best values for the parameters used for the detection of noisy pixels and restoring their values are selected as mentioned in the corresponding literature.

3.5.4 Objective Analysis (*Numerical Results*)

The numerical values in Table 3.4, Table 3.5 and Table 3.6 show the performance comparison obtained by various state-of-the-art filters and proposed technique on selected test images contaminated with different levels of random impulse noise density, in terms of PSNR, SSIM, and FSIM. It is obvious from the results presented in tables that the proposed technique outperformed other benchmark filters in terms of PSNR, SSIM, and FSIM for various noisy images at different levels of noise density. In particular, there is a substantial improvement in the reconstruction process of the impulsive image using the proposed technique as compared with other state-of-the-art filters when noise density exceeds 30%. This can be ascribed to the fact that the large-sized processing window is divided into sub-windows to investigate the presence of noisy pixels while retaining the fine structure of the image.

Detailed graphs in Fig. 3.7 shows the performance comparison of the proposed filter on multiple images contaminated with varying random valued impulse noise density levels in terms of PSNR and SSIM respectively. It can be certainly seen from the evaluation that the proposed filter provides improved performance not only in terms of PSNR i.e., noise elimination but also in terms of SSIM and FSIM i.e., preserving the edges and other fine details present in the image.

3.5.5 Subjective Analysis (*Visual Results*)

The visual quality of the reconstructed images by various state-of-the-art filters and the proposed technique has been demonstrated in Fig. 3.8 and Fig. 3.9. Restoration results of *'Lena'* image contaminated with 40% random valued impulse noise are shown in Fig. 3.8 and Fig. 3.9 shows the restored results of *'Pentagon'* image corrupted

with 50% of random impulse noise. From Fig. 3.8, it can be seen that the proposed filter has recovered the noisy image with improved edge and fine details present in the image. Among all other filters, AFIDM and ATFDF filters worked well for low noise ratio, but as noise density increases, they tend to produce poor results because they are unable to detect and suppress impulsive pixels accurately. Fig. 3.9(i) shows the reconstructed '*Pentagon'* image using the proposed technique. In comparison with other filters, it is observed that the proposed filter recovers the detailed (textural) image perfectly even in the presence of 50% impulse noise. It may be observed that some high-frequency modifications and edge distortions are visible in the output produced by ATFDF and AFIDM filters, but it is not much noticeable in the reconstructed image produced by the proposed filter.

Along with the objective (quantitative) supremacy of the proposed technique established in section 3.5.4, it is apparent from the graphic results of the proposed method that it also has enough noise reduction capability for both low as well as high-density impulse noise besides retaining the fine structure of the image.

To establish the performance of the proposed technique, subjective analysis [45,110] is also performed with respect to human visual perception. The subjective evaluation has been done involving one hundred research students and professionals of our institute on *'Lena'* and *'Pentagon'* images corrupted with 40% and 50% random impulse noise respectively and restored through various state-of-the-art and the proposed filters are shown in Fig. 3.8 and Fig. 3.9. The grading has been carried out by using a rating scale from 1 to 5 representing *Bad, Poor, Fair, Good and Excellent* respectively and tabulated in Table 3.2. The higher count of ratings given by the people has verified the high performance of the proposed filter than that of other filters considered for the subjective evaluation.

Table 3.2: Subjective Analysis of reconstructed images: Rating given by 100 people for *Lena* and *Pentagon* images corrupted with RVIN

Methods	Images	Ratings				
		Bad[1]	**Poor[2]**	**Fair[3]**	**Good[4]**	**Excellent[5]**
DWM [33]	***Lena***	9	20	31	18	22
	Pentagon	12	26	25	20	17
AFIDM [57]	***Lena***	6	13	25	22	34
	Pentagon	8	12	22	28	30
Proposed Method	***Lena***	0	7	19	30	44
	Pentagon	0	6	18	37	39

3.5.6 Time Cost Analysis

We proposed a versatile noise detection and removal scheme in pursuit of accuracy. It may inevitably raise the time cost. The analysis of the time cost is explained next. As the proposed method works in two phases, i.e., the identification and removal phases in an iterative manner, so its overall time cost is a little bit higher. Additionally, time is also consumed in dividing and processing the 5×5 sliding window into 9 overlapped sub-windows (quadrants) of size 3×3.

In the noise identification phase, every pixel of an image is checked whether it is lying in the noisy or noise-free category. For every pixel, 9-quadrants are extracted and then the adaptive threshold is computed through fuzzy inference iteratively that adds to the time cost. In the noise filtering phase, only the identified noisy pixels undergo the noise removal phase by applying simple fuzzy logic-based rules. Hence, more time is consumed in the noise identification phase as compared to the noise removal phase.

Table–3.3 shows the time cost (Seconds) for different images corrupted with varying intensities of RVIN. For the images corrupted with lower intensities of RVIN, the time cost is low, as the proposed filter detects and restore noisy pixel in a single iteration. While for higher intensities of RVIN, more impulsive pixels went through the noise detection and filtering phase in more iterations and hence more time is consumed.

After a thorough analysis, we believe that the extra cost in the detection phase for accuracy is acceptable.

Table 3.3: Time cost (sec) of proposed filter for various images with varying RVIN intensities

Image	RVIN intensity (%)	Time Cost (Sec)
Lena	20	31.80
	40	82.62
	60	84.18
Peppers	20	36.24
	40	84.74
	60	86.38
Bridge	20	34.78
	40	113.30
	60	132.98
Baboon	20	49.61
	40	130.94
	60	132.71

Table 3.4: PSNR values based comparison of the *"Boat"* and *"Bridge"* images degraded with different ratios of RVIN

Image	Methods/ Noise Ratio	TF [69]	NLM [92]	DWM [33]	ACWM [109]	ATFDF [108]	SBF [104]	CEF [102]	SDOOD [101]	MDW [103]	NWM [70]	AFIDM [57]	Proposed Method
Boat	10%	31.41	31.46	33.56	33.43	32.89	32.12	32.55	32.44	32.22	32.54	33.54	**33.56**
	20%	30.01	30.12	31.80	31.41	31.70	30.37	31.20	30.31	30.06	31.48	32.29	**32.39**
	30%	28.45	28.99	29.09	28.57	30.56	28.71	28.50	28.65	28.62	29.24	30.17	**31.13**
	40%	27.70	27.60	27.25	27.13	28.92	27.14	27.19	26.78	26.98	27.66	29.00	**30.38**
	50%	26.79	25.87	25.97	25.49	27.66	26.00	25.65	25.79	26.33	26.34	28.39	**29.40**
	60%	24.91	24.20	24.52	23.76	25.84	24.62	24.15	24.44	24.45	25.18	26.35	**27.69**
Bridge	10%	28.23	**28.63**	28.54	28.00	28.26	27.35	27.89	27.98	28.10	28.02	**28.63**	**28.63**
	20%	27.55	27.34	27.40	27.01	27.37	26.67	26.01	25.56	26.50	26.81	27.34	**27.58**
	30%	24.80	25.74	25.34	24.99	26.15	25.43	23.97	24.34	25.33	25.58	26.41	**26.91**
	40%	23.99	24.19	24.14	23.52	24.95	23.15	22.86	22.59	23.40	24.80	25.75	**26.28**
	50%	22.42	22.85	22.90	22.21	23.89	22.62	21.78	21.69	22.56	23.72	24.32	**25.32**
	60%	21.20	21.22	21.56	20.93	22.48	20.20	20.41	20.57	21.12	22.70	22.89	**23.96**

Table 3.5: SSIM values based comparison of the *"Boat"* and *"Bridge"* images degraded with different ratios of RVIN

Image	Methods/ Noise Ratio	TF [69]	NLM [92]	DWM [33]	ACWM [109]	ATFDF [108]	SBF [104]	CEF [102]	SDOOD [101]	MDW [103]	NWM [70]	AFIDM [57]	Proposed Method
Boat	10%	0.899	0.935	0.933	0.901	0.939	0.912	0.854	0.890	0.911	0.929	0.929	**0.949**
	20%	0.839	0.916	0.891	0.878	0.917	0.886	0.790	0.834	0.891	0.911	0.898	**0.919**
	30%	0.814	0.852	0.855	0.849	0.849	0.826	0.756	0.793	0.854	0.855	0.855	**0.885**
	40%	0.731	0.827	0.816	0.819	0.818	0.764	0.714	0.756	0.822	0.830	0.809	**0.857**
	50%	0.672	0.765	0.737	0.715	0.759	0.719	0.669	0.728	0.778	**0.784**	0.768	**0.784**
	60%	0.639	0.696	0.665	0.579	0.703	0.656	0.609	0.649	0.707	0.736	0.699	**0.738**
Bridge	10%	0.901	0.920	0.897	0.899	0.901	0.874	0.843	0.866	0.900	0.916	0.915	**0.925**
	20%	0.862	0.856	0.828	0.812	0.864	0.822	0.725	0.801	0.826	0.860	0.871	**0.872**
	30%	0.718	0.795	0.786	0.776	0.782	0.699	0.669	0.709	0.795	0.791	**0.812**	**0.812**
	40%	0.617	0.734	0.735	0.725	0.728	0.628	0.625	0.641	0.717	0.740	0.750	**0.757**
	50%	0.556	0.658	0.629	0.638	0.679	0.598	0.550	0.618	0.642	0.663	0.706	**0.707**
	60%	0.492	0.557	0.601	0.482	0.602	0.514	0.484	0.498	0.501	0.607	0.601	**0.615**

Table 3.6: PSNR, SSIM and FSIM values based comparison of the proposed with different filters for images with different ratios of RVIN

Methods		Lena			Pepper			Pentagon		
		40%	50%	60%	40%	50%	60%	40%	50%	60%
TF [69]	*PSNR*	31.36	29.44	27.09	31.02	29.48	27.13	27.81	27.10	26.61
	SSIM	0.866	0.847	0.747	0.681	0.622	0.598	0.696	0.659	0.570
	FSIM	0.951	0.934	0.919	0.901	0.889	0.873	0.932	0.909	0.861
NLM [92]	*PSNR*	32.97	30.02	27.60	31.25	28.94	25.86	27.07	25.63	24.41
	SSIM	0.907	0.860	0.794	0.797	0.722	0.656	0.797	0.747	0.689
	FSIM	0.962	0.945	0.923	0.916	0.910	0.889	0.950	0.929	0.899
DWM [33]	*PSNR*	33.12	32.98	29.76	31.47	30.16	28.39	27.23	26.07	25.69
	SSIM	0.901	0.866	0.775	0.854	0.801	0.782	0.850	0.791	0.649
	FSIM	0.965	0.948	0.910	0.950	0.916	0.870	0.945	0.918	0.882
ACWM [109]	*PSNR*	32.87	31.24	28.80	29.30	27.91	25.82	27.69	26.48	25.01
	SSIM	0.877	0.779	0.589	0.832	0.770	0.662	0.785	0.708	0.595
	FSIM	0.962	0.946	0.903	0.943	0.905	0.865	0.951	0.924	0.882
SBF [104]	*PSNR*	30.78	28.16	26.62	29.54	27.72	25.53	26.34	25.33	22.78
	SSIM	0.889	0.836	0.787	0.798	0.722	0.686	0.755	0.690	0.627
	FSIM	0.969	0.940	0.861	0.916	0.879	0.824	0.917	0.895	0.856
CEF [102]	*PSNR*	31.53	28.69	2590	29.42	27.78	25.21	26.17	25.25	24.11
	SSIM	0.814	0.762	0.709	0.736	0.647	0.589	0.698	0.625	0.565
	FSIM	0.948	0.930	0.922	0.912	0.910	0.894	0.949	0.929	0.903
SDOOD [101]	*PSNR*	32.06	30.24	27.42	30.12	29.31	27.16	25.75	25.09	24.83
	SSIM	0.906	0.869	0.797	0.690	0.644	0.599	0.683	0.653	0.578
	FSIM	0.952	0.942	0.929	0.901	0.886	0.870	0.907	0.895	0.877
DPC-INR [47]	*PSNR*	32.03	30.36	27.65	30.45	30.45	28.45	25.12	24.33	23.59
	SSIM	0.942	0.931	0.872	0.923	0.910	0.872	0.761	0.742	0.661
	FSIM	0.961	0.953	0.931	0.948	0.930	0.906	0.899	0.883	0.871
AFIDM [57]	*PSNR*	35.13	33.69	29.22	31.62	29.76	27.82	30.05	29.11	27.05
	SSIM	0.880	0.846	0.780	0.890	0.856	0.815	0.916	0.895	0.792
	FSIM	0.970	0.952	0.937	0.950	0.938	0.912	0.954	0.937	0.912
Proposed Method	*PSNR*	**35.33**	**34.03**	**32.04**	**33.90**	**32.32**	**29.85**	**30.47**	**29.86**	**28.59**
	SSIM	**0.939**	**0.881**	**0.805**	**0.925**	**0.884**	**0.842**	**0.965**	**0.951**	**0.922**
	FSIM	**0.972**	**0.957**	**0.941**	**0.963**	**0.951**	**0.923**	**0.979**	**0.968**	**0.948**

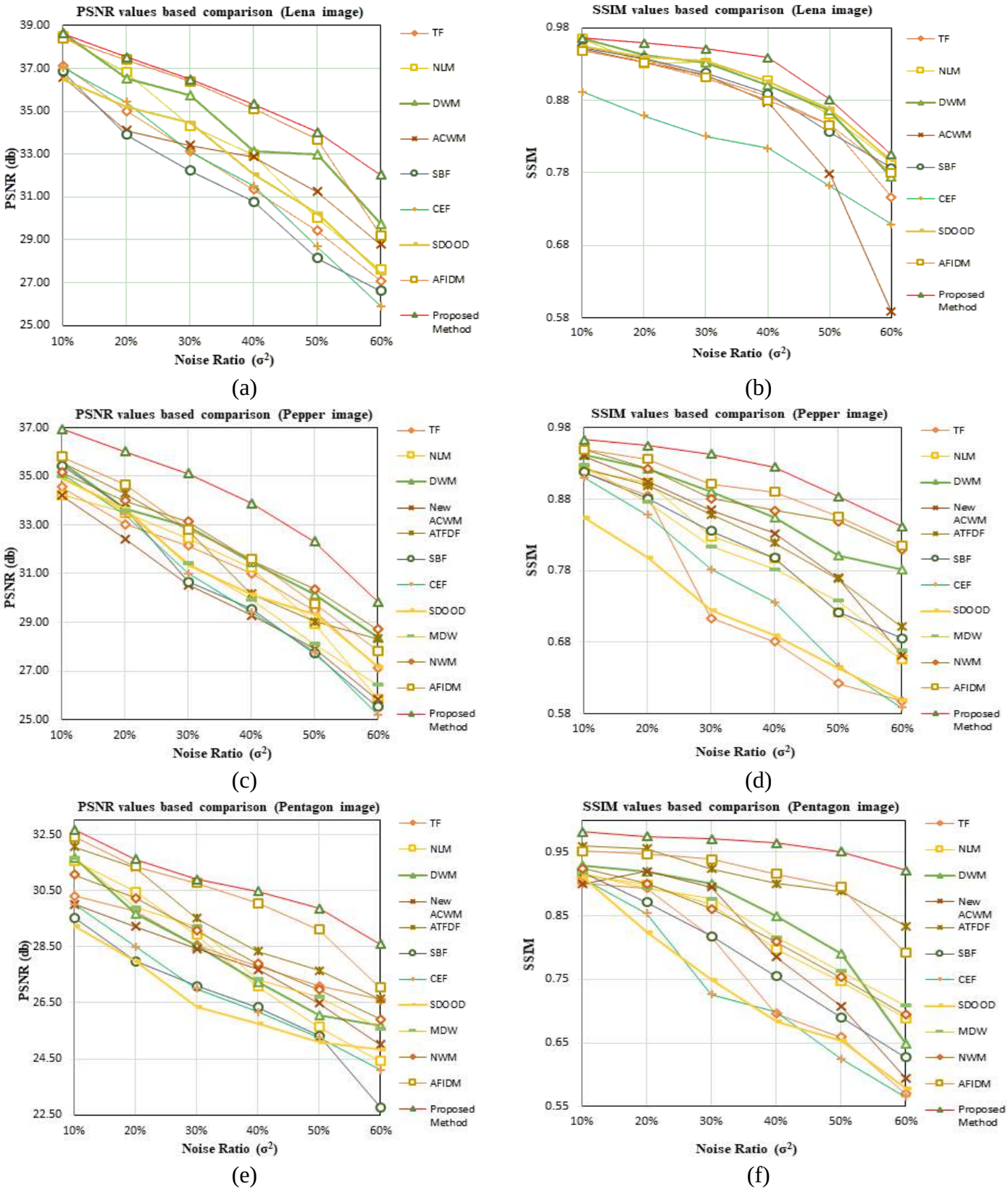

Fig. 3.7: **Graphical Results Analysis:** *PSNR* and *SSIM* based comparison of the proposed technique with benchmarked techniques for (a,b) *Lena* image (c,d) *Pepper* image (e,f) *Pentagon* image respectively

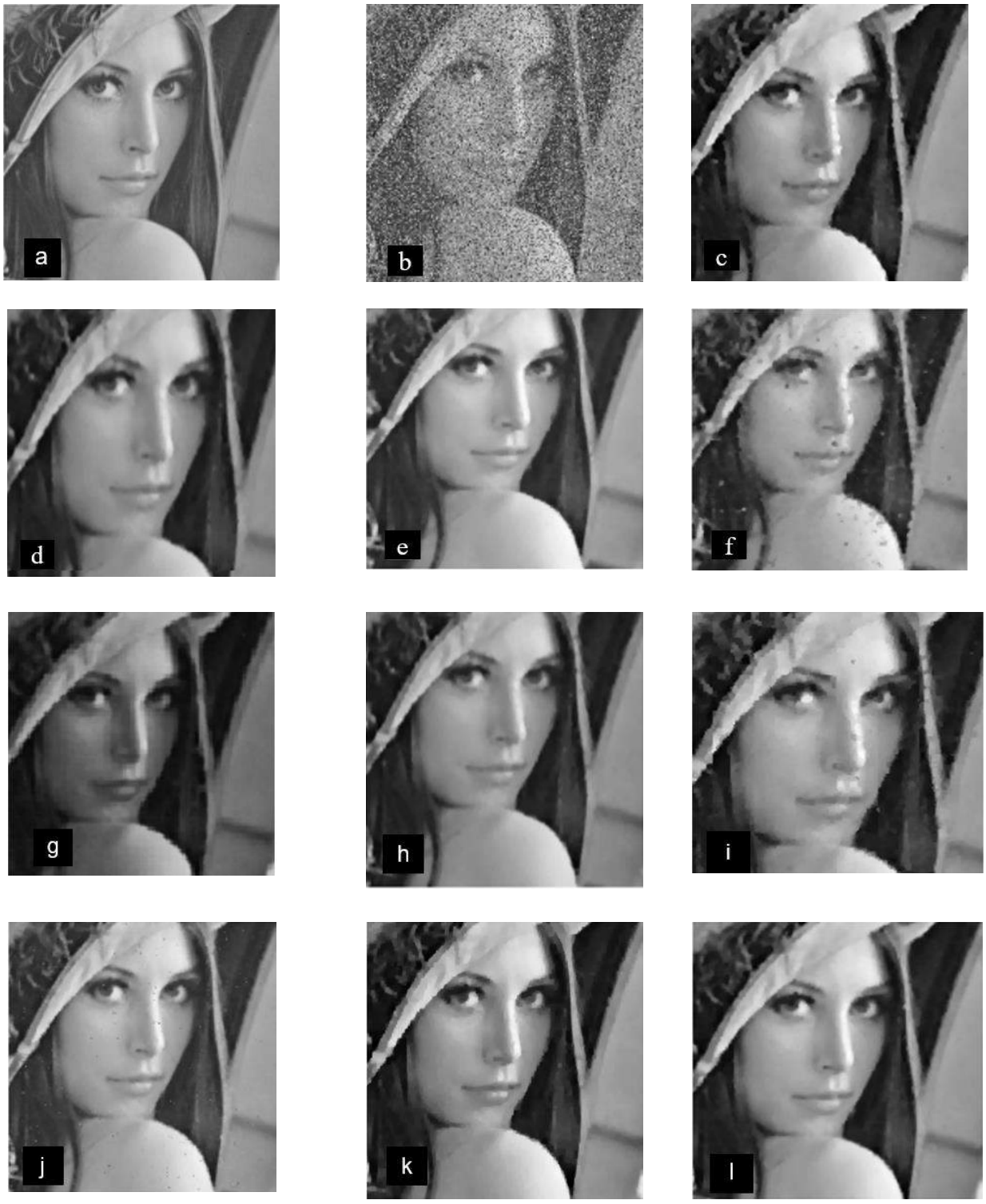

Fig. 3.8: Zoomed Lena images (a) Original (b) Noisy image (40% RVIN). Reconstructed images through (c) NLM, (d) DWM, (e) ATFDF, (f) SBF, (g) CEF, (h) SDOOD, (i) MDW, (j) NWM, (k) AFIDM, (l) Proposed filters

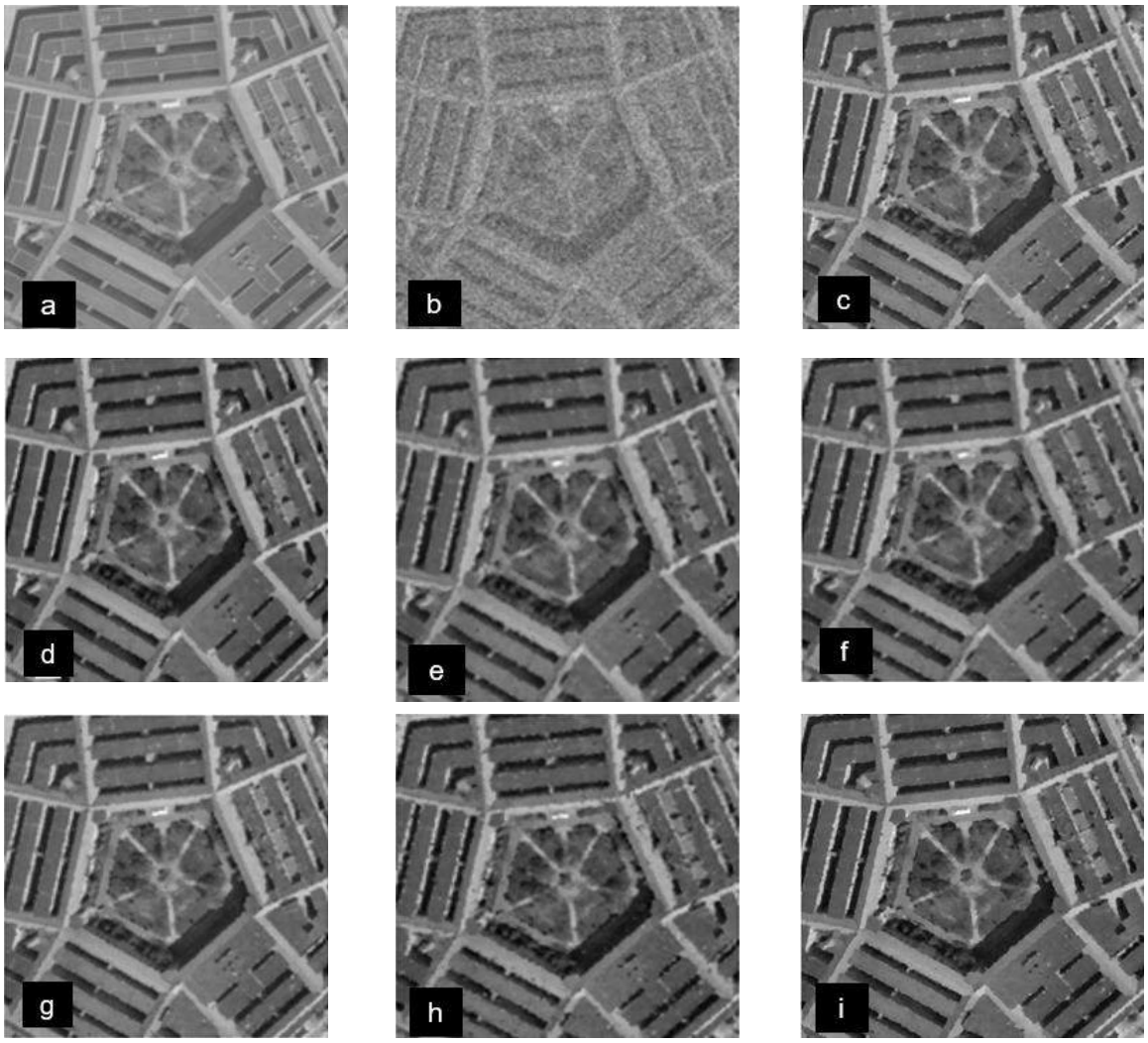

Fig. 3.9: (a) Original Pentagon image (b) Noisy image (50% RVIN). Reconstructed images through (c) NLM, (d)AFIDM, (e) SBF, (f) MDW, (g) NWM, (h) ATFDF, (i) Proposed filters

3.6 Summary

A novel spatial adaptive fuzzy rule-based technique for RVIN reduction from grayscale images has been presented in this chapter. This technique incorporates a hybrid windowing concept, which uses a large-sized window along with its decomposed small-sized sub-windows – *quadrant set* to detect impulsive pixels accurately both in low as well as highly corrupted images. Fuzzy logic based restoration of noisy pixels along with efficient detection technique offers improvement not only in

terms of objective measures but also in terms of visual observation. The simulation results verify that the proposed technique outperforms the other benchmark methods in suppressing the impulse noise while preserving the fine details such as edges and textures of the image even if the noise density is very high.

Chapter 4

Fuzzy Logic based Computational Model for Despeckling Ultrasound Images

Chapter 4

4. Fuzzy Logic based Computational Model for Despeckling Ultrasound Images

In this chapter, a novel filter is proposed that uses local statistics [48] based information for uncertainty modeling based on a computational model – Fuzzy Uncertainty Modelling (FUM) for speckle noise reduction in ultrasound images. The proposed technique [46] uses the concept of fuzzy logic-based uncertainty modeling that analyzes the non-local regions to identify the most "*similar"* ones present in the non-local region of the corrupted pixel. These regions are smoothed by applying local statistics before forwarding to the fuzzy restoration mechanism. This filter creates a balance between the degree of noise removal and edge preservation in an effective way.

Extensive experimentation is performed on synthetic, B-mode simulated and real ultrasonic images to evaluate the performance of the proposed technique both qualitatively and quantitatively and the results are compared with the standard state of the art filters (SRAD [84], SBF [86], NLM [92], OBNLM [93] and NLMLS [39]). Comparative analysis of the results confirmed that the proposed denoising filter performs better than the existing techniques in suppressing the multiplicative noise present in the ultrasound medical images while keeping the image detail intact.

4.1 Contributions

Major contributions of the proposed technique include:

- It acquires the local statistical parameters to find distinct non-local homogenous regions using FUM.
- FUM is used to make a suitable tradeoff between two contradictive objectives, image restoration and structural preservation.

- The proposed fuzzy-based computational model gives superior performance both in terms of despeckling and detail preservation.
- The model is computationally efficient due to less number of multiplications and additions as only similar non-local regions of the image will estimate the restored value of the noisy pixel.

The remainder of this chapter is organized as follows: Section 4.2 presents speckle reduction proposed methodology, explanation of noise estimation and removal process. Experimental setup, results and comparative performance analysis of the proposed technique with the traditional state of the art approaches are described in section 4.3. Finally, the summary of this chapter is presented in section 4.4.

4.2 Methodology

The main objective of the proposed technique is to estimate and eliminate the multiplicative type of speckle-noise from ultrasound medical images while preserving the high-frequency contents that are the edges and fine details. The proposed fuzzy logic and local statistics based NLM technique comprise five modules namely modeling the speckle noise, preprocessing, fuzzy logic based uncertainty modeling, determining the local statistics features and in the last using fuzzy restoration mechanism to recover the speckled pixel. In [38] speckle noise is modeled as a multiplicative in nature. In the preprocessing step, parameters required for noise-free pixel estimation is acquired. In the fuzzy logic-based uncertainty modeling step, a fuzzy-based classifier aid in finding the more "s*imilar non-local regions"* of the contaminated speckled pixel under consideration. These selected "*local and non-local regions*" are first smoothed by applying the local statistical operations before subjecting to the fuzzy restoration module, which uses these processed regions in restoring the value of a speckled pixel. A block diagram of the proposed technique is given in Fig. 4.1.

4.2.1 Speckle noise model

The mathematical model of the speckle noise given in section 2.5 shows that the noise distribution in an ultrasound medical image is signal-dependent and multiplicative in nature.

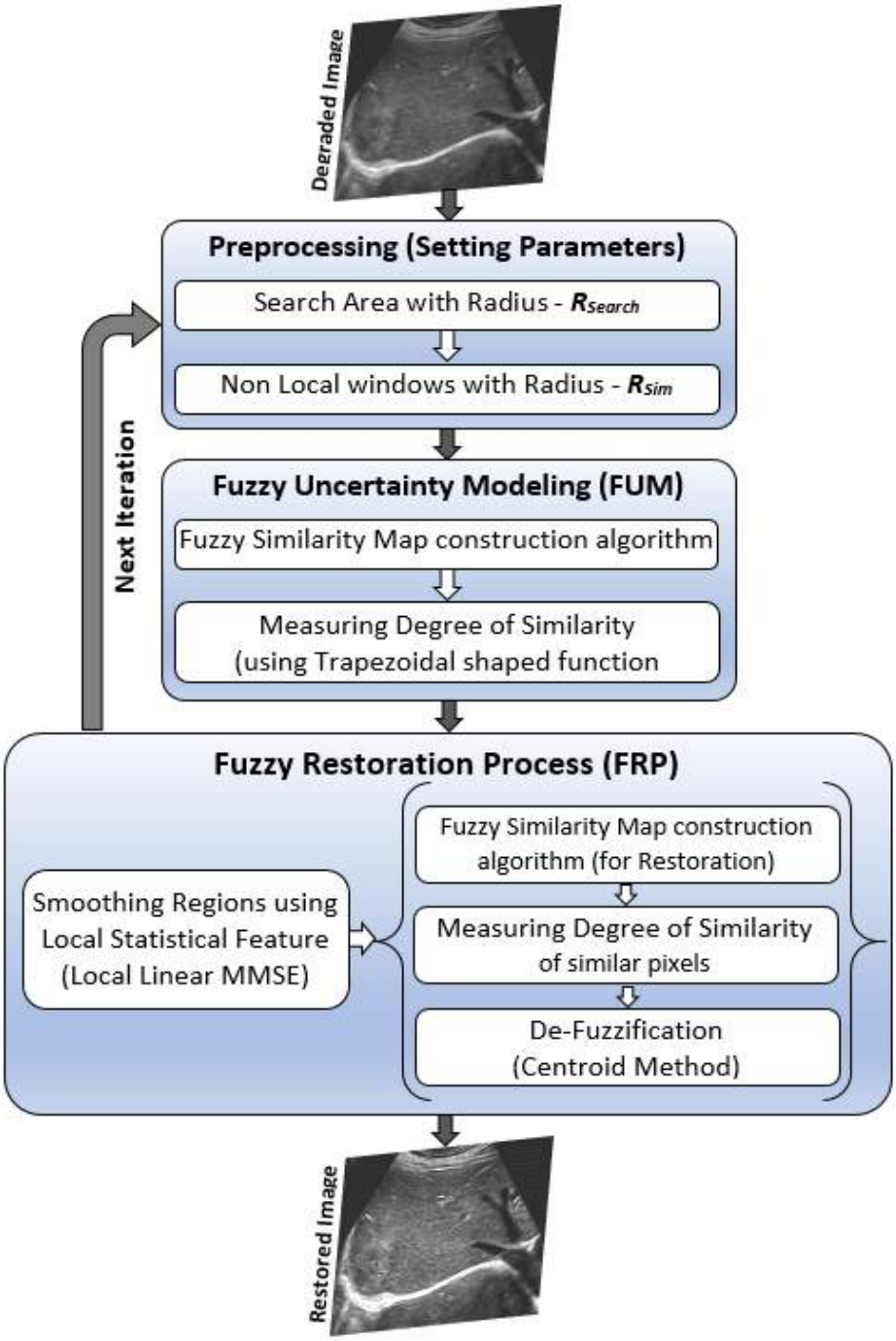

Fig. 4.1: Block diagram of the proposed Speckle reduced filter

4.2.2 Pre-processing module

A smaller size of search window with a radius - R_{search} is convolved round a tainted pixel - $pixel_i$. Fuzzy logic based statistical criteria is applied to find $pixel_j$

similar to $pixel_i$. $R_{similar}$ represent the radius of local and non-local windows W_i and W_j centered at $pixel_i$ and $pixel_J$ respectively. Similarity between $pixel_i$ with all non-local neighboring $pixel_J$ is computed using a region-based comparison method. A detailed procedure is discussed in the coming sections.

4.2.3 Fuzzy logic based Computational Model

In this phase, the *degree of similarity* of window W_i with every non-local window W_j is measured using a fuzzy logic-based mechanism. A reasonably clean pixel can be approximated by looking for similar pixels within the non-local neighborhood. Pixel values of the edges are very different from the other values of the region and normally separate the image into two distinct regions. To estimate the value of noise-free pixels by "*non-local*" neighbors that are not the part of edges present in the image can deform borders of the adjacent regions, which can hinder the diagnose of certain diseases in ultrasonic data. Finding similar patches/regions in the surrounding locality of the central patch W_i is a difficult and challenging job due to the presence of a higher degree of uncertainty in speckled ultrasonic data. A fuzzy rule-based system is used to remove these uncertainties considerably. Two fuzzy membership functions are formed that use mean-ratio R_{μ} and variance-ratio R_{δ^2} of W_i and W_j patches to calculate the degree of membership. These degrees of membership values are then combined to find the overall degree of similarity of the non-local window W_j. Higher the degree of membership, more is the similarity between the local and non-local region, however lower degree means that W_j belong to a different region and therefore the pixels are discarded in the despeckling process. In the fuzzy similarity mechanism, a trapezoidal-shaped fuzzy membership function is used given in Eq. 4.1 and shown in Fig. 4.2.

$$f(x; c_1, c_2, c_3, c_4) = \begin{cases} 0 & if\ x \le c_1 \\ \frac{x-c_1}{c_2-c_1} & if\ c_1 \le x \le c_2 \\ 1 & if\ c_2 \le x \le c_3 \\ \frac{c_4-x}{c_4-c_3} & if\ c_3 \le \mathrm{x} \le c_4 \\ 0 & if\ c_4 \le x \end{cases} \tag{4.1}$$

where $\boldsymbol{x}$ be a vector providing input to the trapezoidal function. Constants $\boldsymbol{c_1}$, $\boldsymbol{c_2}$, $\boldsymbol{c_3}$, and $\boldsymbol{c_4}$ are scalar factors. Here $\boldsymbol{c_1}$ and $\boldsymbol{c_4}$ localize the base of the trapezoidal function, $\boldsymbol{c_2}$ and $\boldsymbol{c_3}$ forms the values of the top.

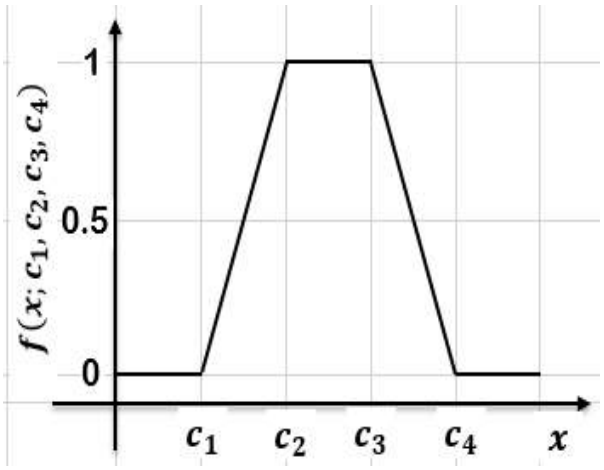

Fig. 4.2: Trapezoidal shaped membership function

The step-by-step process of these factors calculation and measuring the degree of similarity between the two input windows W_i and W_j is described in *Algorithm-1*. All the "*non-local*" regions similar to "*local*" regions are detected in this phase.

Algorithm-1 takes the local window W_i and non-local windows W_j as an input along with three constants, *mean-membership* μ_c, *variance-membership* σ_c^2 and *similarity-threshold* S_t.

The values of constants and threshold depend upon the means and variances of similar and non-similar regions. In the case of speckle-noise removal, these values are set experimentally by analyzing ratios of mean γ_μ and variance γ_{σ^2} defined in section 4.3. Constants μ_c and σ_c^2 are used to set constants $\boldsymbol{c_1}$, $\boldsymbol{c_2}$, $\boldsymbol{c_3}$, $\boldsymbol{c_4}$ and construct two fuzzy membership functions.

Similarity threshold S_t has been used to classify the regions into "*similar*" and "*non-similar*". Regions having a degree of membership greater than or equal to S_t are considered similar and are used by the fuzzy restoration mechanism, however, non-similar patches are simply ignored. The selection of similarity threshold has been made experimentally, value with best results has been given in the experimental results section.

Algorithm 4.1: Fuzzy Logic based Computational Model [50]

Input: Local-Window "W_i", Non-Local window "W_j", constant for Mean-Membership "μ_c", constant for Variance-Membership "σ_c^2" and Similarity-Threshold "S_t"

Output: Decision: Windows are *"Similar"* or *"Not-Similar"*

Begin

1. *Find mean* $-\ \mu_i$ *and variance* $-\ \sigma_i^2$ *of* W_i
2. *Find mean* $-\ \mu_j$ *and variance* $-\ \sigma_j^2$ *of* W_j
3. *Calculate ratio of means* $-\ \gamma_\mu$ *of* W_i *and* W_j, *i.e,* $\gamma_\mu = {}^{\mu_j}/_{\mu_i}$
4. *Calculate ratio of variances* $-\ \gamma_{\sigma^2}$ *of* W_i *and* W_j, *i.e,* $\gamma_{\sigma^2} = {}^{\sigma_j^2}\Big/_{\sigma_i^2}$
5. *Calculate degree of membership* $-\ S_\mu$ *for* γ_μ

   $x = \gamma_\mu, a = 0, b = \mu_c, c = {}^1/_b, d = 1.1 \times c$

   $S_\mu = f(x; a, b, c, d)$
6. *Calculate degree of membership* $-\ S_{\sigma^2}$ *for* γ_{σ^2}

   $x = \gamma_{\sigma^2}, a = 0, b = \sigma_c^2, c = {}^1/_b, d = 1.1 \times c$

   $S_{\sigma^2} = f(x; a, b, c, d)$
7. *Find the Similarity decision:*

   IF $(S_\mu \geq S_t)$ *and* $(S_{\sigma^2} \geq S_t)$ *then*

   Windows are "Similar"

   ELSE

   Windows are "Non-Similar"

   ENDIF

End

4.2.4 Local statistics based noise estimation

Most similar regions W_j identified in the previous section are first smoothed out using local statistical-based noise estimation before subjecting to a fuzzy restoration mechanism for restoration. For estimating noise-free region *f(x)*, Local Linear Minimum Mean Square Error (LLMMSE) [39,82] is used and is given by:

$$\hat{I}_{LLMMSE}(x) = E\big(I(x)\big) + \frac{\delta_I^2(x)}{\delta_N^2(x)}\left[N(x) - E\big(N(x)\big)\right] \qquad (4.2)$$

where $\hat{I}_{LLMMSE}(x)$ is the estimation of noise-free image $I(x)$; $\delta_I^2(x)$ and $\delta_N^2(x)$ are the variances of $I(x)$ and noisy image $N(x)$. E$\big(I(x)\big)$ and E$(N(x))$ are the expectations of ideal image $I(x)$ and input noisy patch $N(x)$ respectively. The values are calculated as described in [82].

4.2.5 Fuzzy Restoration Mechanism

Restored value of a noisy pixel - $pixel_i$ is calculated in this phase by applying local statistical operations on the "*non-local*" regions having a higher degree of similarity with the local region. Similar pixels have identical statistical properties between them. The degree of similarity of the distinct "*local and non-local*" regions are computed using Euclidean distance. Regions having low value have a higher contribution to the noise estimation process and vice versa. Gaussian-shaped fuzzy membership function with zero mean ($\mu = 0$) and estimated noise variance (δ^2) is used to find the involvement of the non-local region W_j.

$$weight(d_{ij}\,;\,\delta,\mu) = e^{\frac{-(d_{ij}-\mu)^2}{2\delta^2}} \tag{4.3}$$

Euclidean distance d_{ij} among the local region '*i*' and non-local region '*j*' is given by:

$$d_{ij} = \|W_i - W_j\| \tag{4.4}$$

The central pixel of patch W_i is also given a weight that is the maximum of all non-local pixel's weights. After weighting all pixels in the search area, the estimated noise-free value of $pixel_i$ is calculated in the defuzzification step using fuzzy centroid technique and is given as:

$$pixel_{\hat{i}} = \frac{1.0}{\sum_{k=1}^{n} weight_k} \sum_{k=1}^{n} (pixel_k \times weight_k) \tag{4.5}$$

The value of $pixel_{\hat{i}}$ gives the estimated restored pixel, *n* represents the count for the non-local similar region and local region. $pixel_k$ is the value of the central pixel of window W_k and $weight_k$ is the weight allocated to the most similar pixel computed using Eq. 4.3.

4.3 Experimental results and discussion

Four different types of tests are carried out to assess the performance of the proposed technique. Experiment-I uses the synthetic data in which noise of different levels is introduced manually. Simulated data is used in Experiments II and III in which the images are generated through the B-mode method applied on ultra-sound simulation [40] and through Field II [111,112] respectively. Real ultrasound images SNR and SSIM metrics explained in section 1.9.1 are computed to gauge the results of the test methods.

The proposed technique is compared with numerous benchmarked filters using these numerical quality measures. The compared filters are SRAD [84], SBF [86], NLM [92], OBNLM [93] and NLMLS [39] which shows good performance over traditional filters like median, Lee, Frost, and Kuan, etc. During the experiments, the number of iterations of the SRAD is kept 500the and for the SBF filter, it is kept 15. The size of the region of NLM, OBNLM and NLMLS and proposed filters is kept *5×5*, search area for these filters is kept *11×11*. The values of the constants in the proposed filter are set experimentally which are:

Mean-Membership "$\boldsymbol{\mu_c}$" = 0.62,
Variance–Membership "$\boldsymbol{\sigma_c^2}$" = 0.19, and
Similarity-Threshold "$\boldsymbol{S_t}$" = 0.70.

4.3.1 Synthetic images (Experiment-I)

To assess the performance of the qualitative and quantitative measures, a synthetic image shown in Fig. 4.3(a) is considered which includes an oval, cardioid, line, triangle and a rectangle. This image is contaminated with different levels of speckle-noise ($\sigma = 0.2, 0.4, 0.6$ and 0.8) for experimentation purposes. A noisy speckled image having variance $\sigma = 0.6$ is shown in Fig. 4.3(b). Restored images obtained after applying various denoised filters are depicted in Fig. 4.3(c)-(h). It can be clearly seen in the denoised images with SRAD and SBF filters shown in Fig. 4.3(c) and (d) that significant noise is still present in the images and fine detail (edge) preservation is not properly maintained. In the case of NLM and OBNLM filters, the over-smoothing effect is clearly visible as shown in Fig. 4.3 (e)-(f). The performance of NLMLS filter is better than others but exhibits many artifacts as shown in Fig. 4.3(g). Fig. 4.3(h)

shows that speckle noise is efficiently reduced and the image retains the original texture well as compared to other state-of-the-art filters.

For quantitative analysis and comparison, SNR and SSIM values of the comparative filters and proposed filter are calculated under different levels of speckle-noise and are listed in Table 4.1. Fig. 4.4 shows the SNR based and SSIM based comparison of filters under different noise levels which shows that the proposed filter has attained maximum SNR up to 75% noise ratio and has approximately equal SNR and SSIM value to NLMLS above 75% noise ratio. This shows that in terms of SNR and SSIM measures, the proposed filter is best and more effective to reduce the speckle noise for synthetic images.

Table 4.1: SNR (db) and SSIM based comparison of different denoising filters on synthetic images contaminated with different levels of speckle noise.

Method	SNR				SSIM			
	0.2	0.4	0.6	0.8	0.2	0.4	0.6	0.8
Noisy image	17.2	11.3	8.3	6.2	0.57	0.31	0.22	0.15
SRAD [84]	28.1	21.9	13.1	8.9	0.95	0.88	0.46	0.26
SBF [89]	20.4	18.3	16.7	15.3	0.88	0.83	0.77	0.70
NLM [86]	27.0	20.0	17.1	15.8	0.93	0.87	0.82	0.78
OBNLM [90]	28.1	21.9	19.4	17.1	0.94	0.92	0.85	0.80
NLMLS [39]	29.0	23.2	20.3	**18.3**	0.96	0.93	0.87	**0.85**
Proposed Filter	**31.0**	**24.1**	**20.8**	**18.3**	**0.97**	**0.94**	**0.88**	**0.85**

4.3.2 B-mode ultrasonic simulated images (Experiment-II)

The effectiveness of different benchmarked despeckled filters and the proposed filter is observed by conducting experimentation on B-mode ultrasonic images. The B-mode simulated image [35] is different from the synthetic image in terms of background which shows different kind of features shown in Fig. 4.5(a). The noisy B-mode simulated image possessing the features of B-scan images is generated in MATLAB by

setting multiple parameters. These are: center frequency of the ultrasonic wave is kept 10e6, the velocity of sound in media is set to 1540m/s, variance of speckle-noise distribution in the image is set to 0.01, pulse-width of the transmitter is 2mm and beamwidth is set to1.5 mm. The original and simulated ultrasound image is shown in Fig. 4.5(a-b). The size of the image is kept *128×128* and is log-compressed for displaying purpose.

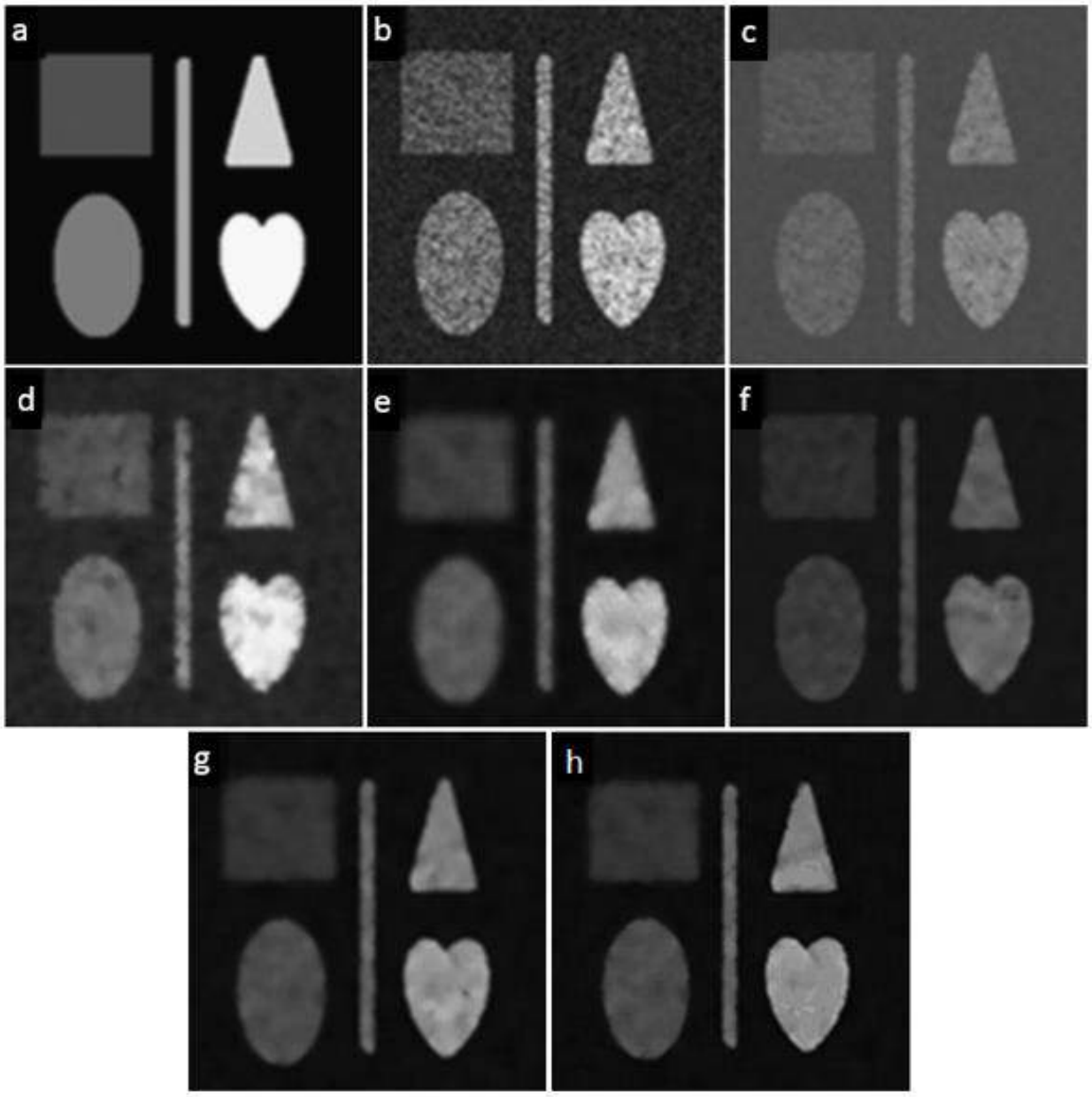

Fig. 4.3: Denoised images obtained from different filters: (a) Original Synthetic image (b) Speckled image with noise δ = 0.6 (c) SRAD (d) SBF (e) NLM (f) OBNLM (g) NLMLS (h) Proposed filter

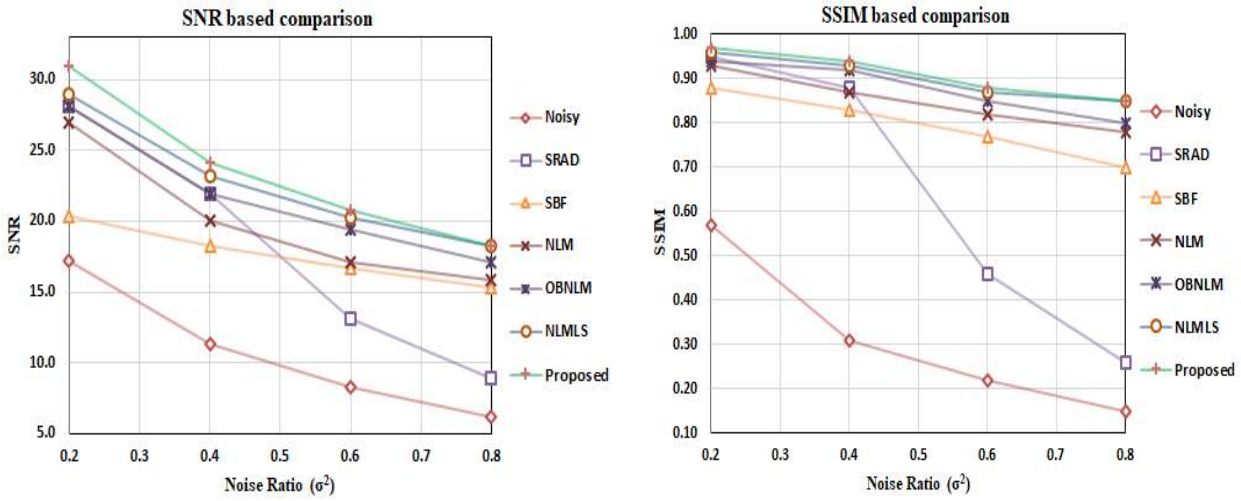

Fig. 4.4: Performance of different denoising filters on synthetic images at different speckle-noise ratios

Table 4.2:

SNR (db) and SSIM based comparison of different denoising filters on B-mode simulated Images contaminated with speckle noise $\delta = 0.6$ (**Experiment-II**)

Method	SNR	SSIM
Noisy image	5.58	0.11
SRAD [84]	5.68	0.33
SBF [89]	5.55	0.33
NLM [86]	5.65	0.37
OBNLM [90]	5.65	0.38
NLMLS [39]	5.67	0.38
Proposed Filter	**9.24**	**0.38**

Table 4.3:

SNR (db) and SSIM based comparison of different denoising filters on Field II simulated images contaminated with speckle noise $\delta = 0.4$. (**Experiment-III**)

Method	SNR	SSIM
Noisy image	8.53	0.12
SRAD [84]	9.41	0.45
SBF [89]	9.12	0.42
NLM [86]	9.51	0.50
OBNLM [90]	9.51	0.50
NLMLS [39]	9.60	0.50
Proposed Filter	**16.59**	**0.54**

Multiple regions shown in the image are regarded as different tissues. Fig. 4.5(b) presents a noisy speckled image with σ = 0.6 and Fig. 4.5(c-h) shows the reconstructed

images after applying SRAD, SBF, NLM, OBNLM, NLMLS, and proposed filters. It is noticeably seen from the restored images obtained after applying these filters that the performance shown is quite unsatisfactory. Moreover, due to the iterative nature of SRAD and SBF filters, they show a negative influence on contrast. The performance of NLMLS and the proposed filter in terms of speckle reduction is very remarkable. But in terms of edge preservation, NLMLS has less accuracy as compared to the proposed filter. The regions in Fig. 4.5(h) are more uniform and close to the original image, edges are more preserved compared to Fig. 4.5(g) which produces blurred edges in the image.

The quantitative values of SNR and SSIM listed in Table 4.2 verifies the best performance of the proposed filter in despeckling B-mode ultrasound images. SNR shows that the proposed technique outperforms and SSIM shows that it is almost the same as that of NLMLS and OBNLM.

4.3.3 Field II kidney simulation (Experiment-III)

In this experiment, the performance of the proposed despeckling filter is evaluated on the simulated *"kidney ultrasonic"* image generated through linear acoustics and Field II program provided by J. A. Jenson [41,111,112]. This program uses the *"Tuphole-Stepanishen"* method to evaluate pulsed ultrasound fields. The kidney data set is more challenging because of the lack of a regularly shaped region. Fig. 4.5 shows the comparison of the existing and proposed filters on Field II kidney simulated image.

Fig. 4.6(a) shows the original and Fig. 4.6(b) presents the noisy image with σ = 0.4. Fig. 4.6 (c-h) shows the reconstructed images after applying SRAD, SBF, NLM, OBNLM, NLMLS and proposed filters respectively. Visual inspection of the results reveal that the SRAD, SBF, NLM, and OBNLM filters tend to over smooth the image; NLMLS and proposed filter produce significant results but Fig. 4.6(h) seems to be more uniform, sharper and retains more fine texture, which proves the best performance of the proposed filter.

The numerical values of SNR and SSIM produced by the comparative and proposed filters are listed in Table 4.3. The high values of SNR and SSIM obtained by the proposed filter (16.59**db** and 0.54) indicate its superiority over other comparative filters in terms of speckle-noise reduction and fine structure preservation capabilities.

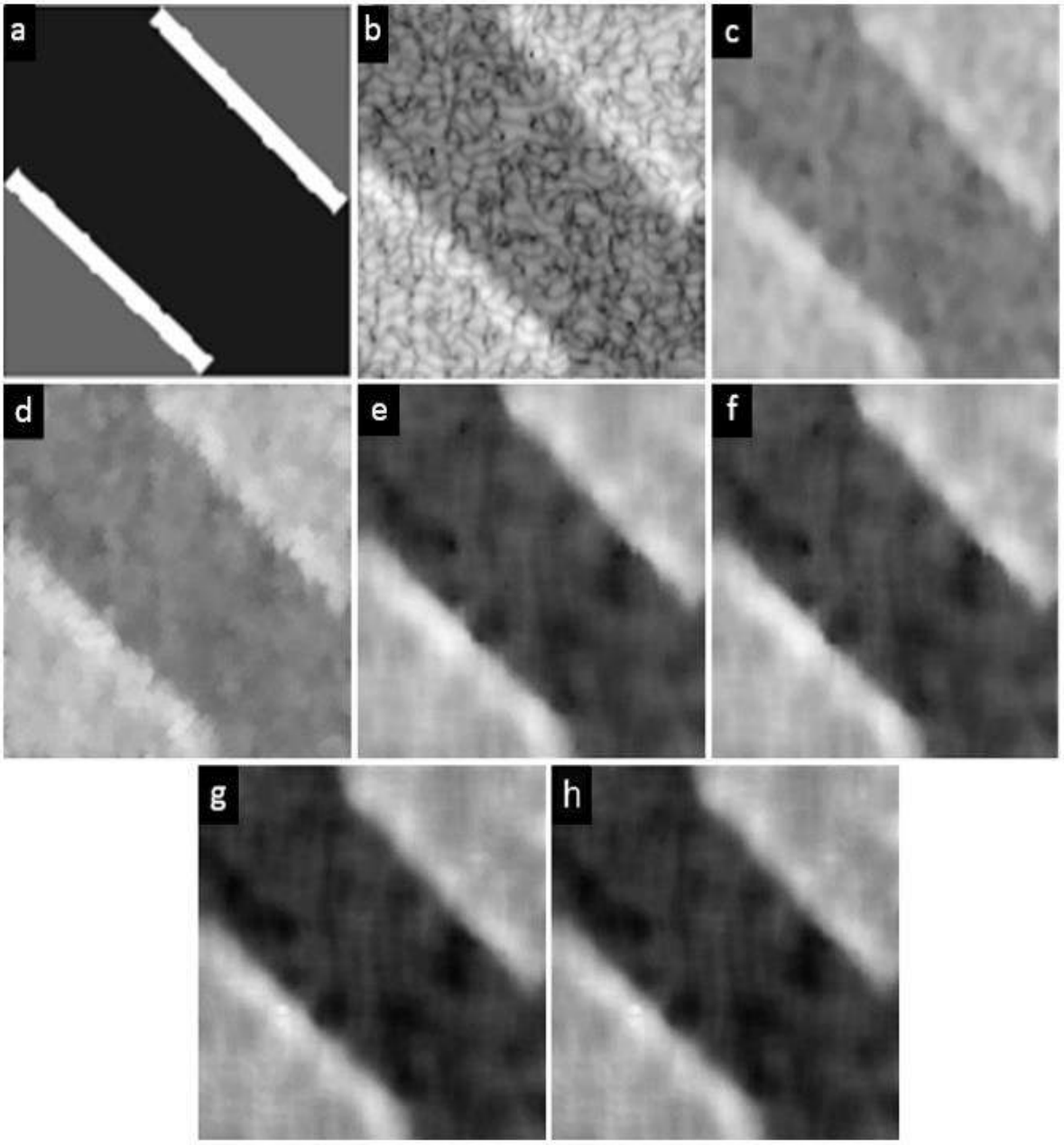

Fig. 4.5: Results of Experiment-II (B-mode simulated image): (a) Original image (b) image with speckle noise $\delta = 0.6$ (c) SRAD (d) SBF (e) NLM (f) OBNLM (g) NLMLS (h) Proposed filter

4.3.4 Real ultrasound images (Experiment-IV)

Filtering the real ultrasound images and evaluating qualitatively is a challenging task because of the characteristics of the acquired signal. Extensive experimentation is performed on the real images of the liver, urinary tract downloaded from "*www.ultrasoundcases.info*". For evaluating the performance of the proposed filter, a

sample speckled image of the liver and the reconstructed images after applying SRAD, SBF, NLM, OBNLM and proposed filters are shown in Fig. 4.7. Visual inspection of the results reveals that the SRAD, SBF and NLM filters shown in Fig. 4.7(b-d) preserves the details but does not remove much noise from the images. OBNLM filter shown in Fig. 4.7(e) removes noise considerably but tends to over smooth the image. Additionally, OBNLN takes long processing time for large size ultrasonic images. The proposed filter produces outstanding results as shown in Fig. 4.7(f) and seems to be more uniform, sharp and retains more fine structural details in small areas of the image.

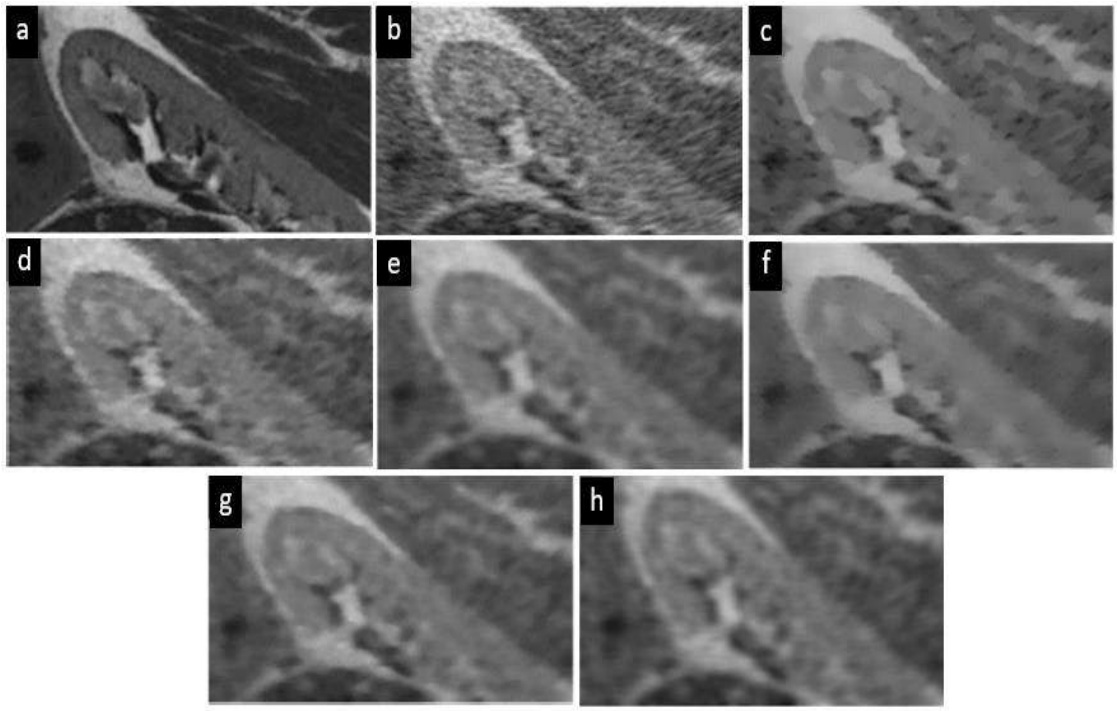

Fig. 4.6: Results of Experiment-III (Field II simulated images): (a) Original image (b) Speckled image with noise δ = 0.4 (c) SRAD (d) SBF (e) NLM (f) OBNLM (g) NLMLS (h) Proposed filter

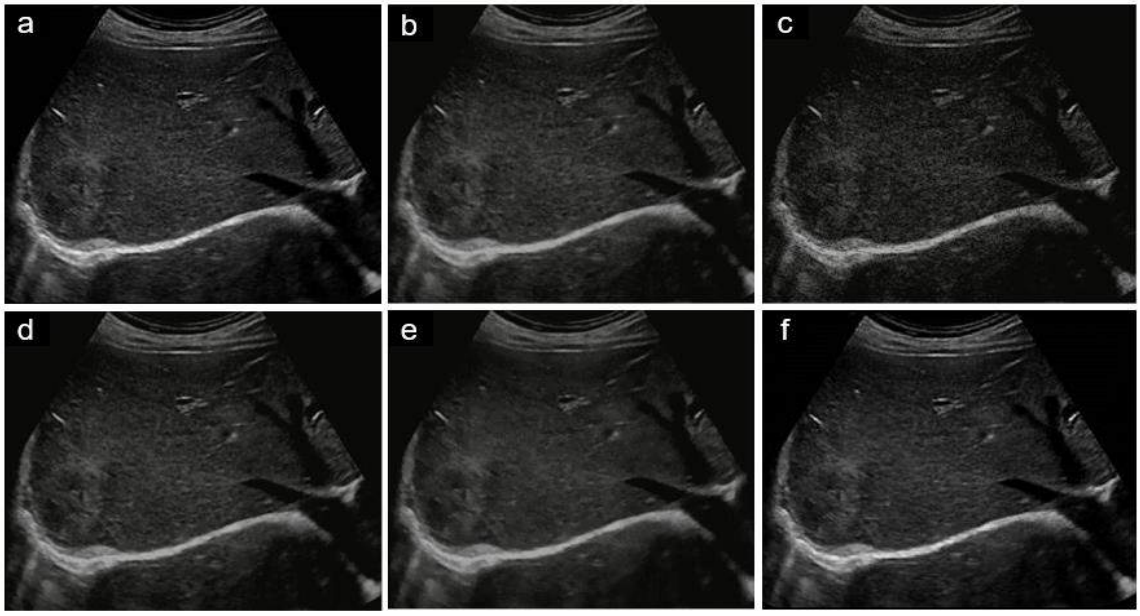

Fig. 4.7: Results of Experiment-IV (real image): (a) Speckled image (b) SRAD (c) SBF (d) NLM (e) OBNLM (f) Proposed filter

4.4 Summary

In this chapter, a novel fuzzy NLM-based filter is proposed for denoising highly speckled ultrasonic images effectively by integrating local and non-local statistical information to figure out the degree of similarity of different regions. The proposed filter not only suppresses the speckle noise considerably but also preserves the fine details and other small structures present in the image in a better way than other speckle reduced filters. Various experiments are conducted on synthetic, simulated and real images to verify the fact. The images are synthesized with different levels of simulated speckle noise. Quantitative and qualitative evaluations are provided to compare the proposed technique with numerous benchmarked filters used for despeckling ultrasound images. The quantitative analysis of the experimental results verifies that the proposed filter exhibits the best despeckling performance in terms of SNR and SSIM values. The human visual assessment suggests that the proposed filter preserves the fine detail and edges present in the small areas of lesions while removing the speckle noise effectively as compared to other benchmarked filtering techniques. In the future, we aim to improve the noise reduction performance of the proposed algorithm so that it can be used in a real-time scenario to assist doctors in the analysis and interpretation of ultrasonic images.

Chapter 5

Conclusions and Future Work

Chapter 5

5. Conclusions and Future Work

5.1 Conclusions

In this dissertation, the restoration of images degraded with impulse noise and speckle noise is studied. In IR, median and NLM filters are considered the most eminent tool for impulse noise and speckle noise removal respectively. Generally, a noise-free image comprises of smooth regions, separated by edges and lines. When filtering operation is applied, we come across two contrary goals, i.e., noise smoothing and edge preservation. Important image details may shatter when smoothing is used for noise removal. Similarly, edge preservation may leave some traces of noise in the restored image. The trade-off between these two conflicting tasks makes the IR problem more demanding and challenging. A mild balance between these two conflicting goals is usually required to develop efficient algorithms. In this regard, two novel filters based on the adaptive fuzzy inference system are proposed.

In chapter 3, a novel spatial adaptive fuzzy rule-based technique for RVIN reduction from grayscale images has been presented. This technique incorporates a hybrid windowing concept, which uses a large-sized window along with its decomposed small-sized sub-windows – *quadrant set* to detect impulsive pixels accurately both in low as well as highly corrupted images. Fuzzy logic based efficient noise detection technique along with effective restoration offers improvement not only in terms of objective (numerical) measures but also in terms of visual observation. The simulation results verify that the proposed technique outperforms the other benchmark methods in suppressing the impulse noise while preserving the fine details such as edges and textures of the image even if the noise density is very high.

In the future, more emphasis may be given on the detection of noisy pixels in the RVIN tainted image to improve the performance of the proposed technique. In

addition, a reduction in time complexity for the detection phase will be given due consideration.

In chapter 4, a novel fuzzy NLM-based filter is proposed for denoising highly speckled ultrasonic images effectively by integrating local and non-local statistical information to figure out the degree of similarity of different regions. The proposed filter not only suppresses the speckle noise considerably but also preserves the fine details and other small structures present in the image in a better way than other speckle reduced filters. Various experiments are conducted on synthetic, simulated and real images to verify the fact. The images are synthesized with different levels of simulated speckle noise. Quantitative and qualitative evaluations are provided to compare the proposed technique with numerous benchmarked filters used for despeckling ultrasound images. The quantitative analysis of the experimental results verifies that the proposed filter exhibits the best despeckling performance in terms of SNR and SSIM values. The human visual assessment suggests that the proposed filter preserves the fine detail and edges present in the small areas of lesions while removing the speckle noise effectively as compared to other benchmarked filtering techniques. In the future, we aim to improve the noise reduction performance of the proposed algorithm so that it can be used in a real-time scenario to assist doctors in the analysis and interpretation of ultrasonic images.

5.2 Future Work

In this thesis, fuzzy logic-based techniques have been used to tackle impulse and speckle noise from general and ultrasonic medical images in the *"spatial domain"*. In the future, this research can be further extended by developing denoising techniques based on fuzzy logic and exploring its use in transform domains.

- In the future, we believe to use other soft computing techniques along with fuzzy logic, as an artificial neural network, particle swarm optimization (PSO), machine learning (ML), etc. to restore impulsive and speckled images.
- In the current study, only two general types of noises that are, impulse and speckle noise have been tackled. In the future, it could be extended to other types of noises as well like Gaussian noise, Rician noise, etc.

- Work can also be extended to deal with colored images along with grayscale images.

References

6. References

[1] M.A. Kitchener, Investigations into image restoration, University of Wollongong, 2012.

[2] R.C. Gonzalez, R.E. Woods, Digital Image Processing, 4th Ed, Pearson Education, 2018.

[3] T. Nodes, N. Gallagher, Median filters: Some modifications and their properties, IEEE Trans. Acoust. 30 (1982) 739–746. doi:10.1109/TASSP.1982.1163951.

[4] S. Siltanen, V. Kolehmainen, S. J rvenp, J.P. Kaipio, P. Koistinen, M. Lassas, J. Pirttil, E. Somersalo, Statistical inversion for medical x-ray tomography with few radiographs: I. General theory, Phys. Med. Biol. 48 (2003) 1437–1463. doi:10.1088/0031-9155/48/10/314.

[5] W.-J. Choi, T.-S. Choi, Genetic programming-based feature transform and classification for the automatic detection of pulmonary nodules on computed tomography images, Inf. Sci. (Ny). 212 (2012) 57–78. doi:10.1016/j.ins.2012.05.008.

[6] S.T. Gandhe, K.T. Talele, A.G. Keskar, Intelligent Face Recognition Techniques: A Comparative Study, GVIP J. 7 (2007) 53–60.

[7] Y. Chen, Phase Insensitive Homomorphic Image Processing for Speckle Reduction, Ultrason. Imaging. 18 (1996) 122–139. doi:10.1006/uimg.1996.0007.

[8] M. Ambrosanio, F. Baselice, G. Ferraioli, V. Pascazio, Ultrasound despeckling based on Non Local Means, in: IFMBE Proc., 2018: pp. 109–112. doi:10.1007/978-981-10-5122-7_28.

[9] Y. Pei, H. Takagi, A survey on accelerating evolutionary computation approaches, in: Proc. 2011 Int. Conf. Soft Comput. Pattern Recognition, SoCPaR 2011, 2011. doi:10.1109/SoCPaR.2011.6089140.

[10] A.J. Mayne, G.J. Klir, T.A. Folger, Fuzzy Sets, Uncertainty, and Information, J. Oper. Res. Soc. (1990). doi:10.2307/2583508.

[11] B. Wilamowski, Neural Networks and Fuzzy Systems, in: Microelectron. 2nd Ed., CRC Press, 2005: pp. 18-1-18–25. doi:10.1201/9781420037593.ch18.

[12] L.A. Zadeh, Fuzzy sets, Inf. Control. 8 (1965) 338–353. doi:10.1016/S0019-9958(65)90241-X.

[13] K.K. Rao, G. SVP Raju, An Overview on Soft Computing Techniques, in: A. Mantri, S. Nandi, G. Kumar, S. Kumar (Eds.), High Perform. Archit. Grid Comput., Springer Berlin Heidelberg, Berlin, Heidelberg, 2011: pp. 9–23.

[14] L. Altenberg, Evolutionary Computation, in: Encycl. Evol. Biol., 2016. doi:10.1016/B978-0-12-800049-6.00307-3.

[15] M. Kubat, An Introduction to Machine Learning, Springer International Publishing, Cham, 2017. doi:10.1007/978-3-319-63913-0.

[16] V. Kolehmainen, S. Siltanen, S. J rvenp, J.P. Kaipio, P. Koistinen, M. Lassas, J. Pirttil, E. Somersalo, Statistical inversion for medical x-ray tomography with few radiographs: II. Application to dental radiology, Phys. Med. Biol. 48 (2003) 1465–1490. doi:10.1088/0031-9155/48/10/315.

[17] J.M. Ollinger, J.A. Fessler, Positron-emission tomography, IEEE Signal Process. Mag. 14 (1997) 43–55. doi:10.1109/79.560323.

[18] J.R. Strub, E.D. Rekow, S. Witkowski, Computer-aided design and fabrication of dental restorations: Current systems and future possibilities, J. Am. Dent. Assoc. (2006). doi:10.14219/jada.archive.2006.0389.

[19] J.J. Winston, D.J. Hemanth, A comprehensive review on iris image-based biometric system, Soft Comput. 23 (2019) 9361–9384. doi:10.1007/s00500-018-3497-y.

[20] Y. Tie, L. Guan, Automatic face detection in video sequences using local normalization and optimal adaptive correlation techniques, Pattern Recognit. 42 (2009) 1859–1868. doi:10.1016/j.patcog.2008.11.026.

[21] K. Cao, A.K. Jain, Automated Latent Fingerprint Recognition, IEEE Trans. Pattern Anal. Mach. Intell. 41 (2019) 788–800. doi:10.1109/TPAMI.2018.2818162.

[22] M.T. Naseem, M. Nadeem, I.M. Qureshi, A. Hussain, Optimal Secure Information using Digital Watermarking and Fuzzy Rule base, Multimed. Tools Appl. 78 (2019). doi:10.1007/s11042-018-6501-8.

[23] S.A. Velastin, Jia Hong Yin, A.C. Davies, Crowd monitoring using image processing, Electron. Commun. Eng. J. 7 (1995) 37–47. doi:10.1049/ecej:19950106.

[24] V.A. Sindagi, V.M. Patel, A survey of recent advances in CNN-based single image crowd counting and density estimation, Pattern Recognit. Lett. 107 (2018) 3–16. doi:10.1016/j.patrec.2017.07.007.

[25] G.L. Charvat, L.C. Kempel, E.J. Rothwell, C.M. Coleman, E.L. Mokole, A through-dielectric radar imaging system, IEEE Trans. Antennas Propag. (2010). doi:10.1109/TAP.2010.2050424.

[26] M.A. Younis, On line surface roughness measurements using image processing towards an adaptive control, Comput. Ind. Eng. 35 (1998) 49–52. doi:10.1016/S0360-8352(98)00017-5.

[27] D. Wei, Image super-resolution reconstruction using the high-order derivative interpolation associated with fractional filter functions, IET Signal Process.

(2016). doi:10.1049/iet-spr.2015.0444.

[28] C.L.P. Chen, H. Li, Y. Wei, T. Xia, Y.Y. Tang, A local contrast method for small infrared target detection, IEEE Trans. Geosci. Remote Sens. (2014). doi:10.1109/TGRS.2013.2242477.

[29] Jie Gui, Dacheng Tao, Zhenan Sun, Yong Luo, Xinge You, Yuan Yan Tang, Group Sparse Multiview Patch Alignment Framework With View Consistency for Image Classification, IEEE Trans. Image Process. 23 (2014) 3126–3137. doi:10.1109/TIP.2014.2326001.

[30] R.H. Chan, Chung-Wa, M. Nikolova, Salt-and-pepper noise removal by median-type noise detectors and detail-preserving regularization, IEEE Trans. Image Process. 14 (2005) 1479–1485. doi:10.1109/TIP.2005.852196.

[31] Y. Dong, R.H. Chan, S. Xu, A Detection Statistic for Random-Valued Impulse Noise, IEEE Trans. Image Process. 16 (2007) 1112–1120. doi:10.1109/TIP.2006.891348.

[32] Chih-Yuan Lien, Chien-Chuan Huang, Pei-Yin Chen, Yi-Fan Lin, An Efficient Denoising Architecture for Removal of Impulse Noise in Images, IEEE Trans. Comput. 62 (2013) 631–643. doi:10.1109/TC.2011.256.

[33] Y. Dong, S. Xu, A New Directional Weighted Median Filter for Removal of Random-Valued Impulse Noise, IEEE Signal Process. Lett. 14 (2007) 193–196. doi:10.1109/LSP.2006.884014.

[34] A. Roy, J. Singha, S.S. Devi, R.H. Laskar, Impulse noise removal using SVM classification based fuzzy filter from gray scale images, Signal Processing. 128 (2016) 262–273. doi:10.1016/j.sigpro.2016.04.007.

[35] F. Ahmed, S. Das, Removal of High-Density Salt-and-Pepper Noise in Images With an Iterative Adaptive Fuzzy Filter Using Alpha-Trimmed Mean, IEEE Trans. Fuzzy Syst. 22 (2014) 1352–1358. doi:10.1109/TFUZZ.2013.2286634.

[36] S. Esakkirajan, T. Veerakumar, A.N. Subramanyam, C.H. PremChand, Removal of High Density Salt and Pepper Noise Through Modified Decision Based Unsymmetric Trimmed Median Filter, IEEE Signal Process. Lett. 18 (2011) 287–290. doi:10.1109/LSP.2011.2122333.

[37] C.T. Lu, T.C. Chou, Denoising of salt-and-pepper noise corrupted image using modified directional-weighted-median filter, Pattern Recognit. Lett. 33 (2012) 1287–1295. doi:10.1016/j.patrec.2012.03.025.

[38] K.Z. Abd-Elmoniem, A.-B.M. Youssef, Y.M. Kadah, Real-time speckle reduction and coherence enhancement in ultrasound imaging via nonlinear anisotropic diffusion, IEEE Trans. Biomed. Eng. 49 (2002) 997–1014. doi:10.1109/TBME.2002.1028423.

[39] J. Yang, J. Fan, D. Ai, X. Wang, Y. Zheng, S. Tang, Y. Wang, Local statistics and non-local mean filter for speckle noise reduction in medical ultrasound image, Neurocomputing. 195 (2016) 88–95. doi:10.1016/j.neucom.2015.05.140.

[40] J.C. Bamber, R.J. Dickinson, Ultrasonic B-scanning: a computer simulation, Phys. Med. Biol. 25 (1980) 463–479. doi:10.1088/0031-9155/25/3/006.

[41] K. Singh, S.K. Ranade, C. Singh, A hybrid algorithm for speckle noise reduction of ultrasound images, Comput. Methods Programs Biomed. 148 (2017) 55–69. doi:10.1016/j.cmpb.2017.06.009.

[42] A. Bovik, Handbook of Image and Video Processing, 1st ed., Elsevier, 2005. doi:10.1016/B978-0-12-119792-6.X5062-1.

[43] K. Gu, S. Wang, G. Zhai, W. Lin, X. Yang, W. Zhang, Analysis of distortion distribution for pooling in image quality prediction, IEEE Trans. Broadcast. 62 (2016) 446–456. doi:10.1109/TBC.2015.2511624.

[44] Lin Zhang, Lei Zhang, Xuanqin Mou, D. Zhang, FSIM: A Feature Similarity Index for Image Quality Assessment, IEEE Trans. Image Process. 20 (2011) 2378–2386. doi:10.1109/TIP.2011.2109730.

[45] A. Roy, R.H. Laskar, Fuzzy SVM based fuzzy adaptive filter for denoising impulse noise from color images, Multimed. Tools Appl. 78 (2019) 1785–1804. doi:10.1007/s11042-018-6303-z.

[46] M. Nadeem, A. Hussain, A. Munir, Fuzzy logic based computational model for speckle noise removal in ultrasound images, Multimed. Tools Appl. 78 (2019) 18531–18548. doi:10.1007/s11042-019-7221-4.

[47] Z. Shi, Z. Xu, K. Pang, Q. Cao, T. Luo, Dissimilar pixel counting based impulse detector for two-phase mixed noise removal, Multimed. Tools Appl. 77 (2018) 6933–6953. doi:10.1007/s11042-017-4613-1.

[48] F. Baselice, Ultrasound Image Despeckling Based on Statistical Similarity, Ultrasound Med. Biol. 43 (2017) 2065–2078. doi:10.1016/j.ultrasmedbio.2017.05.006.

[49] T. Schuster, P. Sussner, An adaptive image filter based on the fuzzy transform for impulse noise reduction, Soft Comput. 21 (2017) 3659–3672. doi:10.1007/s00500-017-2669-5.

[50] M. Sharif, A. Hussain, M.A. Jaffar, T.-S. Choi, Fuzzy-based hybrid filter for Rician noise removal, Signal, Image Video Process. 10 (2016) 215–224. doi:10.1007/s11760-014-0729-1.

[51] M. Habib, A. Hussain, T.S. Choi, Adaptive threshold based fuzzy directional filter design using background information, Appl. Soft Comput. J. 29 (2015) 471–478. doi:10.1016/j.asoc.2015.01.010.

[52] A. Hussain, M. Habib, A new cluster based adaptive fuzzy switching median filter for impulse noise removal, Multimed. Tools Appl. 76 (2017) 22001–22018. doi:10.1007/s11042-017-4757-z.

[53] E. Abreu, S.K. Mitra, A signal-dependent rank ordered mean (SD-ROM) filter-a new approach for removal of impulses from highly corrupted images, in: 1995

Int. Conf. Acoust. Speech, Signal Process., IEEE, 1995: pp. 2371–2374. doi:10.1109/ICASSP.1995.479969.

[54] H.A. David, H.N. Nagaraja, Order Statistics, 3rd Editio, John Wiley & Sons, Inc., Hoboken, NJ, USA, 2003. doi:10.1002/0471722162.

[55] P.J. Huber, E.M. Ronchetti, Robust Statistics, 2nd Editio, John Wiley & Sons, Inc., Hoboken, NJ, USA, 2009. doi:10.1002/9780470434697.

[56] C.C. Kang, W.J. Wang, Fuzzy reasoning-based directional median filter design, Signal Processing. 89 (2009) 344–351. doi:10.1016/j.sigpro.2008.09.003.

[57] M. Habib, A. Hussain, S. Rasheed, M. Ali, Adaptive fuzzy inference system based directional median filter for impulse noise removal, AEU - Int. J. Electron. Commun. 70 (2016) 689–697. doi:10.1016/j.aeue.2016.02.005.

[58] K. Toh, N. Mat Isa, Cluster-based adaptive fuzzy switching median filter for universal impulse noise reduction, IEEE Trans. Consum. Electron. 56 (2010) 2560–2568. doi:10.1109/TCE.2010.5681141.

[59] Tao Chen, Kai-Kuang Ma, Li-Hui Chen, Tri-state median filter for image denoising, IEEE Trans. Image Process. 8 (1999) 1834–1838. doi:10.1109/83.806630.

[60] N.I. Petrovic, V. Crnojevic, Universal Impulse Noise Filter Based on Genetic Programming, IEEE Trans. Image Process. 17 (2008) 1109–1120. doi:10.1109/TIP.2008.924388.

[61] Pei-Eng Ng, Kai-Kuang Ma, A switching median filter with boundary discriminative noise detection for extremely corrupted images, IEEE Trans. Image Process. 15 (2006) 1506–1516. doi:10.1109/TIP.2005.871129.

[62] H. Dawood, H. Dawood, P. Guo, Removal of random-valued impulse noise by local statistics, Multimed. Tools Appl. 74 (2015) 11485–11498. doi:10.1007/s11042-014-2246-1.

[63] A. Roy, L. Manam, R.H. Laskar, Region Adaptive Fuzzy Filter: An Approach for Removal of Random-Valued Impulse Noise, IEEE Trans. Ind. Electron. (2018). doi:10.1109/TIE.2018.2793225.

[64] S. Khan, D.-H. Lee, An adaptive dynamically weighted median filter for impulse noise removal, EURASIP J. Adv. Signal Process. 2017 (2017). doi:10.1186/s13634-017-0502-z.

[65] T. Chen, Hong Ren Wu, Adaptive impulse detection using center-weighted median filters, IEEE Signal Process. Lett. 8 (2001) 1–3. doi:10.1109/97.889633.

[66] S.-J. Ko, Y.H. Lee, Center weighted median filters and their applications to image enhancement, IEEE Trans. Circuits Syst. 38 (1991) 984–993. doi:10.1109/31.83870.

[67] Tao Chen, Hong Ren Wu, Space variant median filters for the restoration of

impulse noise corrupted images, IEEE Trans. Circuits Syst. II Analog Digit. Signal Process. 48 (2001) 784–789. doi:10.1109/82.959870.

[68] V. Crnojevic, V. Senk, Z. Trpovski, Advanced Impulse Detection Based on Pixel-Wise MAD, IEEE Signal Process. Lett. 11 (2004) 589–592. doi:10.1109/LSP.2004.830117.

[69] R. Garnett, T. Huegerich, C. Chui, Wenjie He, A universal noise removal algorithm with an impulse detector, IEEE Trans. Image Process. 14 (2005) 1747–1754. doi:10.1109/TIP.2005.857261.

[70] L. Liu, C.L.P. Chen, Y. Zhou, X. You, A new weighted mean filter with a two-phase detector for removing impulse noise, Inf. Sci. (Ny). 315 (2015) 1–16. doi:10.1016/j.ins.2015.03.067.

[71] S. Khan, D.-H. Lee, An adaptive dynamically weighted median filter for impulse noise removal, EURASIP J. Adv. Signal Process. 2017 (2017) 67. doi:10.1186/s13634-017-0502-z.

[72] Jung-Hua Wang, Wen-Jeng Liu, Lian-Da Lin, Histogram-based fuzzy filter for image restoration, IEEE Trans. Syst. Man Cybern. Part B. 32 (2002) 230–238. doi:10.1109/3477.990880.

[73] S. Schulte, M. Nachtegael, V. De Witte, D. Van der Weken, E.E. Kerre, A fuzzy impulse noise detection and reduction method, IEEE Trans. Image Process. 15 (2006) 1153–1162. doi:10.1109/TIP.2005.864179.

[74] X. Wang, X.Q. Zhao, F.X. Guo, J.F. Ma, Impulsive noise detection by double noise detector and removal using adaptive neural-fuzzy inference system, AEU - Int. J. Electron. Commun. 65 (2011) 429–434. doi:10.1016/j.aeue.2010.06.004.

[75] A. Majid, C.H. Lee, M.T. Mahmood, T.S. Choi, Impulse noise filtering based on noise-free pixels using genetic programming, Knowl. Inf. Syst. (2012). doi:10.1007/s10115-011-0456-7.

[76] S.G. Javed, A. Majid, A.M. Mirza, A. Khan, Multi-denoising based impulse noise removal from images using robust statistical features and genetic programming, Multimed. Tools Appl. 75 (2016) 5887–5916. doi:10.1007/s11042-015-2554-0.

[77] G. Wang, D. Li, W. Pan, Z. Zang, Modified switching median filter for impulse noise removal, Signal Processing. 90 (2010) 3213–3218. doi:10.1016/j.sigpro.2010.05.026.

[78] S. Schulte, V. De Witte, M. Nachtegael, D. Van der Weken, E.E. Kerre, Histogram-based fuzzy colour filter for image restoration, Image Vis. Comput. (2007). doi:10.1016/j.imavis.2006.10.002.

[79] S. Masood, A. Hussain, M.A. Jaffar, T.-S. Choi, Color differences based fuzzy filter for extremely corrupted color images, Appl. Soft Comput. 21 (2014) 107–118. doi:10.1016/j.asoc.2014.03.006.

[80] A. Chaudhry, A. Khan, A. Ali, A.M. Mirza, A hybrid image restoration approach: Using fuzzy punctual kriging and genetic programming, Int. J. Imaging Syst. Technol. 17 (2007) 224–231. doi:10.1002/ima.20105.

[81] V.S. Frost, J.A. Stiles, K.S. Shanmugan, J.C. Holtzman, A Model for Radar Images and Its Application to Adaptive Digital Filtering of Multiplicative Noise, IEEE Trans. Pattern Anal. Mach. Intell. (1982). doi:10.1109/TPAMI.1982.4767223.

[82] D.T. Kuan, A.A. Sawchuk, T.C. Strand, P. Chavel, Adaptive Noise Smoothing Filter for Images with Signal-Dependent Noise, IEEE Trans. Pattern Anal. Mach. Intell. PAMI-7 (1985) 165–177. doi:10.1109/TPAMI.1985.4767641.

[83] J.-S. Lee, Digital Image Enhancement and Noise Filtering by Use of Local Statistics, IEEE Trans. Pattern Anal. Mach. Intell. PAMI-2 (1980) 165–168. doi:10.1109/TPAMI.1980.4766994.

[84] Yongjian Yu, S.T. Acton, Speckle reducing anisotropic diffusion, IEEE Trans. Image Process. 11 (2002) 1260–1270. doi:10.1109/TIP.2002.804276.

[85] K. Krissian, C.-F. Westin, R. Kikinis, K.G. Vosburgh, Oriented Speckle Reducing Anisotropic Diffusion, IEEE Trans. Image Process. 16 (2007) 1412–1424. doi:10.1109/TIP.2007.891803.

[86] P.C. Tay, C.D. Garson, S.T. Acton, J.A. Hossack, Ultrasound Despeckling for Contrast Enhancement, IEEE Trans. Image Process. 19 (2010) 1847–1860. doi:10.1109/TIP.2010.2044962.

[87] J. Kim, J. Hong, H. Park, Prospects of deep learning for medical imaging, Precis. Futur. Med. 2 (2018) 37–52. doi:10.23838/pfm.2018.00030.

[88] A. Maier, C. Syben, T. Lasser, C. Riess, A gentle introduction to deep learning in medical image processing, Z. Med. Phys. 29 (2019) 86–101. doi:10.1016/j.zemedi.2018.12.003.

[89] S.G. Javed, A. Majid, Y.S. Lee, Developing a bio-inspired multi-gene genetic programming based intelligent estimator to reduce speckle noise from ultrasound images, Multimed. Tools Appl. (2018). doi:10.1007/s11042-017-5139-2.

[90] J.J. Nirschl, A. Janowczyk, E.G. Peyster, R. Frank, K.B. Margulies, M.D. Feldman, A. Madabhushi, Deep Learning Tissue Segmentation in Cardiac Histopathology Images, in: Deep Learn. Med. Image Anal., Elsevier, 2017: pp. 179–195. doi:10.1016/B978-0-12-810408-8.00011-0.

[91] K. Zhang, W. Zuo, Y. Chen, D. Meng, L. Zhang, Beyond a Gaussian Denoiser: Residual Learning of Deep CNN for Image Denoising, IEEE Trans. Image Process. 26 (2017) 3142–3155. doi:10.1109/TIP.2017.2662206.

[92] A. Buades, B. Coll, J.-M. Morel, A Non-Local Algorithm for Image Denoising, in: 2005 IEEE Comput. Soc. Conf. Comput. Vis. Pattern Recognit., IEEE, 2005: pp. 60–65. doi:10.1109/CVPR.2005.38.

[93] P. Coupe, P. Hellier, C. Kervrann, C. Barillot, Nonlocal means-based speckle filtering for ultrasound images, IEEE Trans. Image Process. 18 (2009) 2221–2229. doi:10.1109/TIP.2009.2024064.

[94] K. Binaee, R.P.R. Hasanzadeh, A Non Local Means Method Using Fuzzy Similarity Criteria for Restoration of Ultrasound Images, in: 2011 7th Iran. Conf. Mach. Vis. Image Process., IEEE, 2011: pp. 1–5. doi:10.1109/IranianMVIP.2011.6121557.

[95] M. Sharif, A. Hussain, M.A. Jaffar, T.S. Choi, Fuzzy similarity based non local means filter for Rician noise removal, Multimed. Tools Appl. (2015). doi:10.1007/s11042-014-1867-8.

[96] J. Wu, C. Tang, Random-valued impulse noise removal using fuzzy weighted non-local means, Signal, Image Video Process. 8 (2014) 349–355. doi:10.1007/s11760-012-0297-1.

[97] M. Nadeem, A. Hussain, A. Munir, M. Habib, M.T. Naseem, Removal of random valued impulse noise from grayscale images using quadrant based spatially adaptive fuzzy filter, Signal Processing. 169 (2020) 107403. doi:10.1016/j.sigpro.2019.107403.

[98] T.C. Lin, Switching-based filter based on Dempster's combination rule for image processing, Inf. Sci. (Ny). 180 (2010) 4892–4908. doi:10.1016/j.ins.2010.08.011.

[99] Bo Xiong, Zhouping Yin, A Universal Denoising Framework With a New Impulse Detector and Nonlocal Means, IEEE Trans. Image Process. 21 (2012) 1663–1675. doi:10.1109/TIP.2011.2172804.

[100] G.R. Arce, J.L. Paredes, Recursive weighted median filters admitting negative weights and their optimization, IEEE Trans. Signal Process. 48 (2000) 768–779. doi:10.1109/78.824671.

[101] A.S. Awad, Standard Deviation for Obtaining the Optimal Direction in the Removal of Impulse Noise, IEEE Signal Process. Lett. 18 (2011) 407–410. doi:10.1109/LSP.2011.2154330.

[102] U. Ghanekar, R. Pandey, A.K. Singh, A Contrast Enhancement-Based Filter for Removal of Random Valued Impulse Noise, IEEE Signal Process. Lett. 17 (2010) 47–50. doi:10.1109/LSP.2009.2032479.

[103] Z. Li, G. Liu, Y. Xu, Y. Cheng, Modified directional weighted filter for removal of salt & pepper noise, Pattern Recognit. Lett. 40 (2014) 113–120. doi:10.1016/j.patrec.2013.12.022.

[104] Chih-Hsing Lin, Jia-Shiuan Tsai, Ching-Te Chiu, Switching Bilateral Filter With a Texture/Noise Detector for Universal Noise Removal, IEEE Trans. Image Process. 19 (2010) 2307–2320. doi:10.1109/TIP.2010.2047906.

[105] S. Schulte, V. De Witte, M. Nachtegael, D. Van Der Weken, E.E. Kerre, Fuzzy Two-Step Filter for Impulse Noise Reduction From Color Images, IEEE Trans.

Image Process. 15 (2006) 3567–3578. doi:10.1109/TIP.2006.877494.

[106] S. Schulte, V. De Witte, M. Nachtegael, D. Van der Weken, E.E. Kerre, Fuzzy random impulse noise reduction method, Fuzzy Sets Syst. 158 (2007) 270–283. doi:10.1016/j.fss.2006.10.010.

[107] E.E. Kerre, Introduction to the basic principles of fuzzy set theory and some of its applications, 2nd ed., Communication & Cognition, 1991.

[108] A. Hussain, M.A. Jaffar, A.M. Mirza, C. Asmatullah, Detail preserving fuzzy filter for impulse noise removal, Int. J. Innov. Comput. Inf. Control. 5 (2009) 3583–3591.

[109] T.-C. Lin, A new adaptive center weighted median filter for suppressing impulsive noise in images, Inf. Sci. (Ny). 177 (2007) 1073–1087. doi:10.1016/j.ins.2006.07.030.

[110] Q. Huynh-Thu, M.N. Garcia, F. Speranza, P. Corriveau, A. Raake, Study of rating scales for subjective quality assessment of high-definition video, IEEE Trans. Broadcast. 57 (2011) 1–14. doi:10.1109/TBC.2010.2086750.

[111] J.A. Jensen, FIELD: A program for simulating ultrasound systems, Med. Biol. Eng. Comput. 34 (1996) 351–352.

[112] J.A. Jensen, N.B. Svendsen, Calculation of pressure fields from arbitrarily shaped, apodized, and excited ultrasound transducers, IEEE Trans. Ultrason. Ferroelectr. Freq. Control. 39 (1992) 262–267. doi:10.1109/58.139123.

[113] K.N. Plataniotis, A.N. Venetsanopoulos, Adaptive Image Filters. In: Color Image Processing and Applications, Digital Signal Processing. Springer, Berlin, Heidelberg (2000).

[114] P. A. Vikhar, "Evolutionary algorithms: A critical review and its future prospects," 2016 International Conference on Global Trends in Signal Processing, Information Computing and Communication (ICGTSPICC), Jalgaon, pp. 261-265, (2016).